

UNIVERSITY OF AMSTERDAM

MASTERS THESIS

Mathematically Modeling the Interactions Between Phages, Bacteria, and the Environment

Author:

Victor PIASKOWSKI

Examiner:

Dr. Jaap Kaandorp

Supervisor:

Dr. Matti Gralka

Assessor:

Dr. Yuval Mulla

*A thesis submitted in partial fulfillment of the requirements
for the degree of Master of Science in Computational Science*

in the

Computational Science Lab
Informatics Institute

June 2025

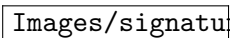
clslogo.png

Declaration of Authorship

I, Victor PIASKOWSKI, declare that this thesis, entitled ‘Mathematically Modeling the Interactions Between Phages, Bacteria, and the Environment’ and the work presented in it are my own. I confirm that:

- This work was done wholly or mainly while in candidature for a research degree at the University of Amsterdam.
- Where any part of this thesis has previously been submitted for a degree or any other qualification at this University or any other institution, this has been clearly stated.
- Where I have consulted the published work of others, this is always clearly attributed.
- Where I have quoted from the work of others, the source is always given. With the exception of such quotations, this thesis is entirely my own work.
- I have acknowledged all main sources of help.
- Where the thesis is based on work done by myself jointly with others, I have made clear exactly what was done by others and what I have contributed myself.

Signed:

re.pdf

Date: June 23, 2025

“All models are wrong, but some are useful”

George E. P. Box

UNIVERSITY OF AMSTERDAM

Abstract

Faculty of Science
Informatics Institute

Master of Science in Computational Science

**Mathematically Modeling the Interactions Between Phages, Bacteria, and
the Environment**

by Victor PIASKOWSKI

In any given microbial ecosystem, there can be hundreds of different phages and bacteria interacting with one another in a complex system. These individual interactions have a significant impact on the bacterial community and the overall ecosystem, with important ecological consequences. They force bacteria to mutate and evolve, changing the community fitness level. Phages can control bacterial populations, ensuring that dangerous bacteria do not over-reproduce and harm the ecosystem. Phages control bacterial population dynamics using the “kill-the-winner” dynamic, preventing any one species from dominating. Upon lysis, bacteria release resources into the environment that other bacteria and plants can use.

There is a need to mathematically model complex systems, but current models typically only model 1 or 2 phages and bacteria. It is, however, straightforward to extend the model to multiple species. Mathematically modeling large bacterial communities is important because running lab experiments takes time and is costly. These simulations can guide future lab work, for example, in combating antibiotic-resistant bacteria.

I created a program consisting of three parts that can model complex communities of p phages, b bacteria, and r resources. The first part uses a GUI tool to create and edit the interactions between the phages, bacteria, and resources using a graph network. The nodes and edges hold the interaction and environmental parameter values. The second part, the simulation framework itself, models and calculates the phage, bacteria, and resource population levels with the user-provided network and ODE model. The third part allows the user to interact with the simulation framework with a custom-built dashboard. The user can, for example, change the parameter values from the dashboard and immediately see how the change affects the simulation. There are five pre-built plots that the user can interact with. It is possible to download the simulation results so that the user can create custom analyses and plots.

I apply this process to the Golding model from Geng et al. [1]. I qualitatively analyze the model’s behavior and use a SOBOL analysis to quantitatively assign a value to the model’s variance in output from the model’s input. In addition, understanding the different regimes of restriction in phages, as well as the factors that drive reaction rates and determine the rate-limiting steps, is crucial. By varying the initial uninfected bacteria population, the model can interpolate between two limiting scenarios, adsorption and latency limited. It is important to determine whether a phage population will proliferate in a laboratory context under constant washout to prevent the phage population from accidentally being wiped out. I run an analysis to see if phages will proliferate or die out depending on the initial condition. Finally, I perform and analyze a co-existence analysis on a large 20-phage, 20-bacteria, and 10-resource community to determine whether

phages and bacteria can coexist under various conditions. I find that in large communities, phages and bacteria can coexist. If a debris term is introduced, the bacteria's survivability rate increases.

Acknowledgements

I would like to thank my parents for loving me despite some of my faults, and for supporting me through my Bachelor and Master studies even if they don't exactly know what I am studying. Without them, I wouldn't know where my life would be right now, and I certainly would be a different person if it were not for them.

Thank you to Dr. Matti Gralka for the weekly meetings and teaching me everything about phages and bacteria. Every meeting was always insightful, productive, and informative. I will forever be amazed at how he can remember which paper talks about which topic, and how he always had a paper for every topic.

Thank you to Sofia Blaszczyk for finding the Master thesis opening and suggesting that I email Dr. Gralka for an introductory meeting. She acted as my rubber duck programming buddy, and watched my cringe screen recordings that I sent her at 2am showcasing various demos of my project. If she wouldn't have found this opening, I wouldn't know what I would be doing as my thesis.

If I hadn't followed Dr. Rik Kaasschieter's and Dr. Martijn Anthonissen's courses "Introduction Computational Sciences" and "Numerical Linear Algebra" in my Bachelors, I would not have been interested in Computational Sciences. I would not have found the MSc Computational Sciences program, as Computational Sciences fits my interests and skill sets better than any other program I could have taken. For Rik and Martijn have forever altered my career trajectory.

Thank you to Sarah Flickinger for showing me the research that she has been doing in the lab. She allowed me to really connect my research and models to real life, reminding me that what I am doing has real life use cases than just a purely theoretical or programming challenge.

And finally, thank you to all of my friends for keeping me sane and helping me through both of my programs.

Contents

Declaration of Authorship	i
Abstract	iii
Acknowledgements	vi
Contents	vii
List of Figures	xi
List of Tables	xiv
Abbreviations	xv
1 Introduction	1
1.1 Thesis Overview	1
1.2 The Environment	2
1.3 Biological Background	2
1.3.1 Phage's Role in the Environment	3
1.3.1.1 Phages and Controlling Bacterial Blooms	3
1.4 Phage Cocktails and Human Health	4
1.5 Potential Applications of Phages	4
1.6 Modelling Phages in a Complex Community	4
1.7 Software Overview	5
2 Literature review	7
2.1 Methods of Modelling Phages and Bacteria	7
2.1.1 Generalized Lotka-Volterra Model	8
2.1.2 Generalized Consumer-Resource Model	8
2.2 Phage Biology	9
2.2.1 What Are Phages?	9
2.2.2 How Does the Phage Cycle Work?	9
2.3 Bacterial Defense Against Phages	10
2.3.1 Mutations in Bacterial DNA (Genetic (Co-)Evolution)	10
2.3.2 Horizontally Transferring DNA	11

2.3.3	Phage Inactivation and Decoys	11
2.3.4	Phenotype Resistance	11
2.3.5	Spatial Refuge/Biofilms	11
2.4	Phage Counter Defense Against Bacteria	12
2.4.1	Genetic Mutations	12
2.4.2	Viral Recombination	12
2.5	Phage Defense Against Phages	13
2.5.1	Altering Cell Structure	13
2.5.2	Protein Creation	13
2.5.3	Growth Curves Typically Seen in a Lab	13
2.6	Bacteria and Phages in the Lab	14
2.6.1	Running Experiments	15
2.6.2	Chemostats	15
2.6.3	Petri Dishes	15
2.6.4	Measuring Growth	16
2.6.5	Serial Transfer	16
2.7	Software Mathematically Modelling Phages, Bacteria, and Resources . . .	17
2.7.1	Cocktail	17
2.7.2	PhageDyn	17
2.7.3	Cocktail and PhageDyn Limitations	18
2.8	The Golding Model	19
2.8.1	The Original Golding Model	19
2.8.2	The Adapted Golding Model	20
3	Methods	21
3.1	Project Overview	21
3.1.1	Network Creation Tool	21
3.1.2	Simulation Framework	22
3.1.3	Visualization Dashboard	23
3.1.3.1	Editing Network and Parameter Values	24
	Initial Condition	24
	Vector Data	24
	Matrix Data	24
	Environment and settings	24
3.1.3.2	Visualization and Analysis	24
	Serial Transfer	26
	Parameter Analysis	26
	Initial Value Analysis	27
	Phase Portrait	28
	SOBOL Sensitivity Analysis	29
	Ultimate Analysis	30
3.1.4	Custom Visualizations and Analyses	31
3.2	Software Used and Packages	32
4	Experiments and Results	33
4.1	SOBOL Sensitivity Analysis Results	33
4.1.1	Resources	34

4.1.2	Phages	34
4.1.3	Total Bacteria	35
4.1.4	Results	35
4.2	Graph Behavior with IVA	35
4.3	Initial Value Analysis Results	37
4.4	Phage Proliferation	38
4.4.1	Phase Portrait	38
4.4.2	An Initial Phage and Resource Analysis for Phage Proliferation . .	39
4.4.3	An Initial Phage, Bacteria, and Resource Analysis for Phage Pro- liferation	39
4.5	Plotting Parameter Change — $3 \times 2 \times 3$ Model	41
4.6	Phage and Bacteria, Survivability Analysis For A $20 \times 20 \times 10$ System . .	42
5	Discussion	44
5.1	Graph Behavior	44
5.2	A Realistic Growth Curve	45
5.3	SOBOL Sensitivity	45
5.3.1	Resources	46
5.3.2	Phages	46
5.3.3	Total Bacteria	47
5.4	Initial Value Analysis	48
5.5	Phage Proliferation	49
5.5.1	Phase Portrait	49
5.5.2	3D Plot	50
5.6	Plotting Parameter Change	50
5.7	Large $20 \times 20 \times 10$ System	50
6	Conclusion and Future Work	52
6.1	Conclusion	52
6.2	Future Work	53
6.2.1	Other Models	53
6.2.1.1	Model Replication	54
6.2.1.2	Debris	55
6.2.1.3	Spatial simulations	55
	PDE	55
	Discretization	55
6.2.2	Lab Work	56
6.2.2.1	Environmental Modelling	56
7	Ethics and Data Management	58
7.1	Ethical Considerations	58
7.2	Data Management	58
7.3	Adherence to Codes and Principles	59
A	Appendix A: Equation Parameters	60
A.1	Simple/Advanced Golding Model Parameters	60

A.2	SOBOL Parameters	60
A.3	Linear Regression Parameters	60
B	Appendix B: Industrial and Real Life Applications of Phages	63
B.1	Controlling Foodborne Bacteria	64
B.1.1	Current Applications	64
B.2	Phage Therapy and Antibiotics	66
B.2.1	Current Applications: Bacterial Infection Control	66
B.3	Environmental Protection	67
B.3.1	Current Applications	68
C	Appendix C: Flowchart of User and System Interactions	70
D	Appendix D: ODE Model Implementation	72
E	Appendix E: Parameter Values Used	73
E.1	Realistic Growth Curves	73
E.2	A Second Realistic Growth Curve	73
E.3	SOBOL Analysis	73
E.4	Complex Model	73
F	Appendix F: Extra Plots and Figures	76
F.1	SOBOL Analysis With Washin and Washout	76
F.1.1	Final Value Analysis	76
F.1.1.1	Resources	76
F.1.1.2	Phages	76
F.1.1.3	Total Bacteria	76
F.1.2	Peak Value and Time of peak	77
F.2	Why 95%?	77
F.3	Varying r and β In A $3 \times 2 \times 3$ System	79
	Bibliography	84

List of Figures

1.1	Life cycle of a phage, inside and outside a bacteria cell. Significant steps in the life cycle of a phage include the infection stage, integration, replication, and lysing process. Figure sourced from Campbell [2].	3
2.1	Different models and how the bacterial entities interact with itself, one another, resources and the environment. All figures sourced from van den Berg et al. [3]	8
2.2	Parts of a phage, a real life picture of phages infecting an <i>E. coli</i> bacterium, and an artist's impression of phages infecting a bacterium.	9
2.3	Growth population of a $1 \times 1 \times 1$ system. The log plot allows to see behavior happening at values approaching and to plot data on a logarithmic scale. The parameters used for this plot can be found in Table E.1.	14
2.4	Bacteria lawn, the dots on the petri dish show no bacteria growth due to the presence of phages. Photo courtesy of S. Flickinger.	16
2.5	Example output from Cocktail and PhageDyn respectively. For PhageDyn, concentration of heterotrophic biomass in an aerobic plug flow across four situations. See Nilsson [4] and Krysiak-Baltyn et al. [5] for more information on parameter values and supplementary resources.	18
3.1	This network topography along with a $1 \times 1 \times 1$ network will be used in the Chapter 3 and Chapter 4 sections. The parameter values for the networks can be found at Table E.1, Table E.4 and Table E.3 Each node represents a phage, bacteria, or resource, with arbitrary interactions occurring between them. Although not shown and used here, edges between the same entity types and self loops are allowed.	22
3.2	The tabs where the user can edit the various parameter values and control the simulation parameters	25
3.3	Serial Transfer	26
3.4	Parameter Analysis	27
3.5	The IVA settings and output.	28
3.6	Phase portrait settings and output.	28
3.7	SOBOL variance analysis settings and output.	30
3.8	The ultimate analysis setup tab.	31
4.1	SOBOL analyses for the final, peak, and time of peak value, without a washin and washout rate. The input value ranges to test each parameter used for this SOBOL test can be found in Table E.3, except washin and washout is 0.	37

4.2	Varying the initial uninfected bacteria concentration, from 50 to 500, with 30 unique values tested. Varying the default parameter values a can have a large influence on how changing the initial bacteria concentration influences the dynamics of the system. The default values for Figure a) and b) can be found at Table E.1 and Table E.2.	38
4.3	Varying initial resources and initial phages and the resulting proliferation and fitted proliferation curve. The box is colored red if the phages proliferated for that condition, and white if the phages died out. Phages proliferated if they reached 2 times their initial population at any point in time in the simulation. This simulation used the values from Table E.2, but with washout set to 0.02 instead of 0.	40
4.4	3D plot of phage proliferation, dependent on initial resource, uninfected bacteria, and phage population. Color scaling from white to red, color is dependent on the max phage population reached.	41
4.5	Varying r , β , and ω^o . All phage values set to 10 to show how the network connections and vector/matrix values affect phage growth. Selectively chosen sub-figures from Figure F.3, Figure F.4, and Figure F.5. Chosen parameter values can be found in Table E.4.	43
4.6	The output graph for the default parameter values for a large $20 \times 20 \times 10$ network. Parameter values were randomly chosen in the interval given by Table E.3.	43
5.1	A large $20 \times 20 \times 10$ model with a debris model added. The debris parameter values were randomly and uniformly selected between 0.01 and 0.2.	51
6.1	Exponential growth curve vs logistic growth	54
B.1	SalmoLyse [®] reduces Salmonella contamination on various food surfaces: Mean and standard error bars shown. Statistical analyses were carried out for each food group independently. Asterisks denote significant reduction from corresponding controls based on one-way ANOVA with Tukey's post-hoc tests for multiple corrections: ** denotes $p < 0.01$, while *** denotes $p < 0.001$ compared to the corresponding controls. There was significant reduction in Salmonella on all food surfaces with the addition of SalmoLyse [®] compared to the controls; the mean percent reductions from the control are noted in the boxes above treatment bars. CFU/g D colony forming units per gram. Each letter denotes a food group that was tested with SalmoLyse [®] and compared to a control: A= chicken; B= lettuce; C= tuna; D= cantaloupe; E= ground turkey. Plot sourced from Soffer et al. [6].	65
B.2	<i>Salmonella</i> count in a mixture of 5 <i>Salmonella</i> strains spot-inoculated (CFU/g) onto a) lettuce and b) sprouts after spraying with a mixture of bacteriophage (SalmoFresh TM) relative to positive controls at 2, 10 and 25C and stored for 1, 24, 48 and 72 h. Plot sourced from Zhang et al. [7]	65
B.3	Cyanobacteria degradation cycle, main hazards of cyanobacteria bloom to water bodies, aquatic organisms, and the human body. (DO: dissolved oxygen; SD: water transparency; Cond: conductivity; N: nitrogen; P: phosphorus; MCs: microcystins). [8]	68

C.1	The flowchart of user and system interactions. Read from top to bottom.	71
E.1	The parameters used for this plot can be found in Table E.1.	74
F.1	SOBOL analyses for the final, peak, and time of peak value with a washin and washout rate. The data was saved from the dashboard and plotted using Matplotlib. The values used for this SOBOL test can be found in Table E.3.	78
F.2	Testing the 95% rule vs the 100% rule, where the time at the absolute peak is taken and plotted in the second plot. A comparison of phages and uninfected bacteria is shown. Verification of the graph shape between the 95% rule graph and a frequent time step with 100% rule can be seen between c) and e). The e value is changed, ranging from 0.05 to 0.25. . .	80
F.3	Washout $\omega^o = 0$	81
F.4	Washout $\omega^o = 0.02$	82
F.5	Washout $\omega^o = 0.05$	83

List of Tables

4.1	A table that compares how moving one individual parameter value up or down relative to Figure 2.3a changes the general shape of the curve. Reference parameter values used to compare the produced curves are included in the parentheses, taken from Table E.1.	36
A.1	Golding model parameters with variables, names, and descriptions. Subscripts on parameters indicate relationships; for example, e_{br} is nonzero if there is an edge connecting bacteria b to resource r in the network, zero otherwise.	61
A.2	SOBOL parameter symbols, name, and description.	61
A.3	Variable symbol, name, and description used for the linear regression. . .	62
E.1	The parameter values used for Figure 2.3.	73
E.2	Another set of realistic growth curves. The linear and logarithmic plot of this data can be seen in Figure E.1	74
E.3	The parameter values used for the SOBOL sensitivity analysis in Figure 4.1 (SOBOL analysis without washin and washout) and Figure F.1 (SOBOL analysis with washin and washout). For SOBOL analysis with washin and washout, there are $2^{15}(9+2) = 425984$ unique simulations run.	75
E.4	The parameter values used for the $3 \times 2 \times 3$ network model rounded to 5 decimal points. If there is no edge between a phage, bacteria, or resource, then in the matrix representation of the parameter, 0 is stored as the default value.	75

Abbreviations

DDE	D elay D ifferential E quation
DNA	D eoxyribo N ucleic A cid
GUI	G raphical U ser I nterface
IC	I nitial C ondition
IVA	I nitial V alue A nalysis
OD	O ptical D ensity
ODE	O rdinary D ifferential E quation
PA	P arameter A nalysis
PDE	P artial D ifferential E quation
RNA	R ibo N ucleic A cid
ST	S erial T ransfer
UA	U ltimate A nalysis
UvA	U niversitiet v an A msterdam

Chapter 1

Introduction

Phages are small viruses on the order of 27-190nm that infect and lyse (kill) specific bacteria. Phages act as nature's anti-microbial defense, but also impact bacteria evolution and resource turnover. There are various medical and industrial applications for phages to control bacterial growth, but to realize these applications, it is important to know how phages and bacteria interact with one another in order to implement a robust method to control bacterial growth.

1.1 Thesis Overview

This thesis covers multiple topics to ultimately answer how phage, bacteria, and resource interactions with one another and the environment can be mathematically modelled. To answer this question, I wrote a simulation framework that can model and interact with any $p \times b \times r$ system, p phages, b bacteria, and r resources. Using the software, I answer how phages impact community dynamics in complex microbial communities.

First, there is a biological introduction to phages and bacteria. This introduction covers how phages infect bacteria, how bacteria defend against phages, how phages defeat bacterial defenses, and how phages defend against other phages. There is an introduction to different methods of modelling phages and bacteria dynamics. This thesis briefly covers software that models phages, resources, bacteria, and their limitations.

This thesis presents software I developed to support the research, demonstrating its capabilities using a representative model of phage, bacteria, and resource interactions. The section also provides an overview of its usage, including example outputs from demonstration runs. I use the software to analyze various scenarios, such as phage proliferation under a washout scenario and analyze growth rate-limited regions.

1.2 The Environment

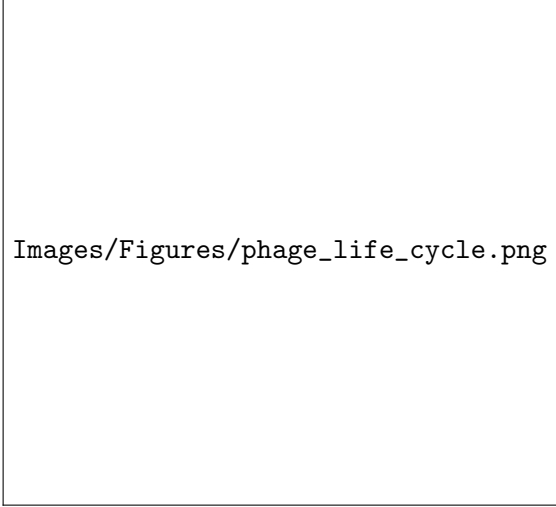
In an ecosystem like the ocean, the gut, or in soil, there are thousands of different microbes all interacting with one another or the surrounding environment. The interactions are complex, with many factors affecting the growth of bacteria and phages.

The interactions between entities in the environment are often synergistic. When an animal dies, bacteria start to digest and decompose the animal into simpler chemicals like carbon and nitrogen that plants can use to grow, which is then eaten by other animals. External factors, such as flooding, droughts, chemical spills, or introduction of new entities have a massive impact on the ecosystem. These events can add or remove resources from the system, change environmental parameters such as the surrounding temperature, introduce competition, or create an imbalance in the population by killing entities. These effects have a larger effect on the ecosystem and food chain as a whole as bacteria are one of the fundamental foundations for resource recycling.

1.3 Biological Background

Phages are small viruses on the order of 27-190nm (the average size of marine phages are 54nm) that infect and lyse (kill) specific bacteria. The phage cycle process starts with a phage coming into contact with a bacterium Figure B.3. Once it has identified an injection site, the phage can inject a strain of DNA into the bacteria. The DNA strand has two options. The first option is that the phage can enter the lysogenic cycle by merging into the host cell's DNA. Prophages are phages that have integrated with the host cell's DNA. As the bacteria replicate, the new cell will also include the prophage's DNA already integrated into the cell's DNA. The second option is that the phage immediately enters the lytic cycle by immediately hijacking the DNA replication process in order to create copies of the phage DNA.

The phage will leave the lysogenic cycle after leaving a signal, for example after the cell receives damage, and hijack the DNA replicating mechanism. The phage will create multiple copies of itself, using the transcription and translation machinery of the host to create multiple copies of itself. The phages self-assemble inside the bacteria until they lyse the cell (e.g., through chemically induced rupture of the cell wall), releasing the phages into the environment.



Images/Figures/phage_life_cycle.png

Figure 1.1: Life cycle of a phage, inside and outside a bacteria cell. Significant steps in the life cycle of a phage include the infection stage, integration, replication, and lysing process. Figure sourced from Campbell [2].

1.3.1 Phage’s Role in the Environment

Phages play a large role in the ecosystem. As bacteria die, for example through lysis, they release resources into the environment for other bacteria and plants to use. This turns over resources like nitrogen and carbon for other sources to use. Phages also help mediate horizontal gene transfer, disperse pathogenic diseases, and spread antibiotic resistance [9]. Phages directly alter bacteria population diversity and population fitness by introducing new ways for bacteria to mutate [10]. There are about 10^6 bacteria cells/ml and 10^7 phages/ml of marine water. About 5% of any bacteria are currently infected and about 15% of daily bacterial death can be attributed to phages [11].

Phage populations grow by infecting their hosts, but they can also degrade, e.g., by UV. UV is a large factor of deactivating marine phages, causing up to a 5% reduction in phage infectivity per hour [11].

1.3.1.1 Phages and Controlling Bacterial Blooms

Phages could potentially be used to control *Cyanobacteria* (blue-green algae) blooms in the environment [12]. *Cyanobacteria* cause damage to aquatic life by consuming resources and oxygen, starving aquatic life and negatively affect human health. There is hope that phages can be used to biologically control water quality in waste water treatment plants and in the environment without the use of harsh chemical processes what would otherwise pose environmental and health hazards [5, 13]. More information about controlling *Cyanobacteria* can be read in Appendix B.3.

1.4 Phage Cocktails and Human Health

There is particular interest in phage applications in human and animal health, called phage therapy. There are about 100 trillion microbes across 5,000 different types of bacteria strains in the human gut. The phages will target the specific bacteria of interest, for example *E. Coli*, but it will not affect the other bacteria found in the gut of the human body. Antibiotics indiscriminately affect any bacteria disrupt the intricate ecosystem of the gut microbiome, acting as a scorched-earth mechanism. Antibiotics have also faced the challenge that bacteria are growing resistance to it, making the antibiotic less effective in the future [14, 15]. Phages on the other hand specifically target a specific bacterial strain. Antibiotic resistant bacteria are typically less resistant to phages. The bacteria cell typically has a trade-off between antibiotic resistance and phage resistance. So by designing phages to be highly infective, there is hope that the phage-resistant bacteria will lose the antibiotic resistance to counter the phages [16, 17]. Appendix B.2 goes more in depth on how phages can be used in a healthcare setting.

1.5 Potential Applications of Phages

Phages have many uses in an industrial setting. Similarly, phage therapies can be used as a preventative method, by preventing the spread of common bacteria in livestock by dosing the animal feed with the phage pills. Farmers often raise livestock in tight spaces with a lack of sanitation facilities, increasing the risk of a disease spreading.

Phages can be used to control the growth of bacteria like *Salmonella* while producing food in a factory [6, 18]. Appendix B.1 in Appendix B goes into more detail about using phages to control foodborne bacteria.

1.6 Modelling Phages in a Complex Community

What we know about phages mechanistically often comes from well researched bacteria in a lab like *E. coli* and its phages, and what we know about phages in the environment comes from metagenomic surveys. Making the connection between the mechanistically and metagenomic models, which would allow us to make and test different models, is the difficult part. Because of this, we need mathematical models to help bridge the gap between the lab and the environment.

There have been previous attempts to model the complex dynamics of the populations between phages, bacteria, and resources, with the environment using Ordinary Differential Equations (ODE) and Delay Differential Equations (DDE). Not every interaction in the complex community can be identified, and if an interaction has been identified, the associated parameter values need to be experimentally derived.

There are two main ways to model phage-bacteria dynamics: spatially and non-spatially. In a spatial model phages and bacteria can move through space and interact with their neighbors. Partial differential equations (PDE) and cellular agent-based models (ABM) have been used to model spatial interactions. Spatial models lead to more computationally complex models, but can result in more biologically realistic results.

By contrast, ODE and DDE models describe non-spatial models. In a non-spatial model, the bacteria and phages are assumed to be in a well-mixed solution and no distinctions are made in regard to neighbors or distances to other entities. Interactions are simplified to a probabilistic approach, where a percentage p of entities interact with one another at time step t . Non non-spatial models are easier to develop, understand, and are more effective in modeling large populations, at the cost of losing spatial information.

For this thesis, the focus will be modelling resource, phage, and bacteria interactions using an ODE model. A phage-bacteria-resource system is described as an $p \times b \times r$ system, meaning p phages, b bacteria, and r resources. Current modelling methods have mainly stayed with $1 \times 1 \times 1$ models, meaning 1 phage, 1 bacteria, and 1 resource. This thesis aims to develop a simulation framework that can model any $p \times b \times r$ ODE system.

1.7 Software Overview

The project is divided into three logical parts, with an optional fourth part. The first section is to create the network interaction. Here the user of the software can define the number of resources, phages, and bacteria, who interacts with who, and the strength and type of interactions. See Section 3.1.1 for further information. In Section 3.1.2, the user uploads the network model and parameters and as output receives the time data and population data as an array. Section 3.1.3 allows the user to interact with Section 3.1.1 and Section 3.1.2 with a dashboard. The user can graphically edit the attribute values of the edges and nodes of the network, and the user can run more advanced visualizations, for example by changing a parameter value and seeing how that affects the population count. There are a few plots included out of the box that the user can test. The plots offered in part 3 offer interactivity like hiding and showing lines and dots, zooming in and out, and hovering over the lines and dots to show more details of the data.

Finally, the user can optionally run multiple simulations and download the data to their disk to create their own custom visualizations using Section 3.1.4. The visualizations created in Section 3.1.3 can theoretically be recreated in Section 3.1.4. The user can choose the same parameter values used for a specific plot in Section 3.1.3, run the simulation (under the Section 3.1.3.2 section), download the data, and reimplement the graphs.

The user can use the tool themselves by importing the Python classes in their own code and initializing the classes and passing the appropriate data.

Chapter 2

Literature review

2.1 Methods of Modelling Phages and Bacteria

The most common way to model phages, bacteria, and resources populations and interactions is with Ordinary Differential Equations (ODEs) or Delay Differential Equations (DDE). DDEs are similar to ODEs, but DDEs incorporate time delays to account for processes that depend not only on the current state but also on past states, to incorporate behavior that has a delay, like latent infection time.

One way to introduce a delay in an ODE model is to force populations to go through stages, causing a delay in other events. For example, in the paper Geng et al. [1], infected bacteria go through M stages of infection, before lysing. By decreasing τ (the latent period) in the model proposed by Geng et al. [1], more infected bacteria go from infected state i to infected state $i + 1$ per timestep, causing the infected peak population count to peak earlier.

The ODE method is simple to understand and easy to set up, but it can only capture large population dynamics. Certain assumptions about the community interactions also have to be made, such as that everything is a probabilistic approach. Each model can be further developed, for example by adding temperature and pH dependence, bacteria releasing nutrients, or phage resistance.

2.1.1 Generalized Lotka-Volterra Model

The Lotka-Volterra model, a first-order non-linear differential model, captures the dynamics between predators and prey. Any population can be modelled as such:

$$\frac{dB_i}{dt} = B_i \left(\left(r_i + \sum_j^N \alpha_{ij} B_j \right) - m_i \right)$$

where r_i is reproduction rate, α_{ij} is the devour rate of B_i on B_j . If α_{ij} is negative, then B_i has a negative effect on B_j , otherwise B_i has a positive effect on B_j . m_i is the removal rate of B_i . The interactions can be seen in Figure 2.1a.

It is possible to add phages into the system by

2.1.2 Generalized Consumer-Resource Model

The generalized Consumer-Resource Model models the growth of a population and resource dynamics between a population of bacteria B_i and a resource R_i .

$$\frac{dB_i}{dt} = r_i B_i \left(\sum_{\alpha} \Delta w_{i\alpha} C_{i\alpha} R_{\alpha} \right) - m_i B_i \quad (2.1)$$

$$\frac{dR_{\beta}}{dt} = - \sum_i C_{i\beta} R_{\beta} B_i + \sum_{\alpha, i} D_{\beta\alpha}^i C_{i\alpha} R_{\beta} B_i \quad (2.2)$$

$$\Delta w_{i\alpha} = \sum_{\beta} D_{\beta\alpha}^i w_{\beta}$$

Equation (2.1) describes the growth of population B_i and Equation (2.2) describes the resource dynamics and metabolism of resource R_{β} . Resource R_{α} can become resource R_{β} at rate $R_{\beta\alpha}^i$. Bacteria B_i reproduces at rate r_i dependent on the concentration of resources $\sum_{\alpha} C_{i\alpha}$. Bacteria die out at rate m_i . For a visual, see Figure 2.1b

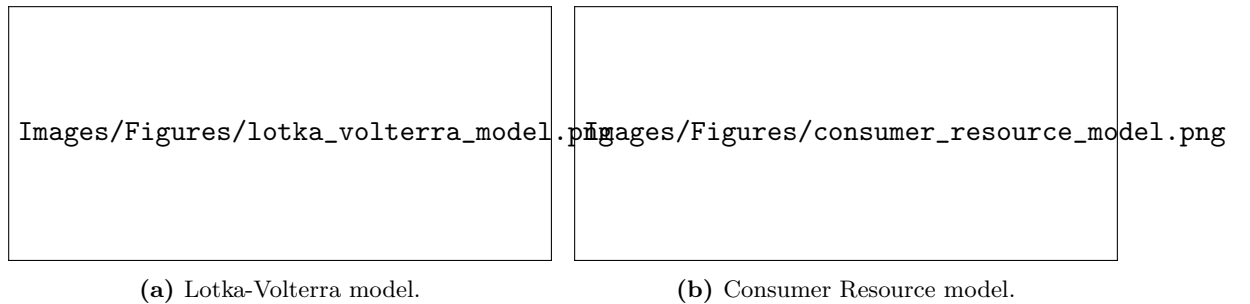


Figure 2.1: Different models and how the bacterial entities interact with itself, one another, resources and the environment. All figures sourced from van den Berg et al. [3]

2.2 Phage Biology

2.2.1 What Are Phages?

Phages are small bundles of proteins that contain viral DNA. Phages are made up of multiple parts built like LEGO to complete the task of infecting a bacterium. Figure 2.2a shows the body parts of a phage. The aim of the phage is to find a suitable bacterial host and infect the host with viral DNA. The DNA alters the host's metabolic pathways to its benefit and hijacks the cellular replication process to create new copies of the phage. Eventually, the cell lyses, releasing the newly created phages into the environment to infect more bacteria.

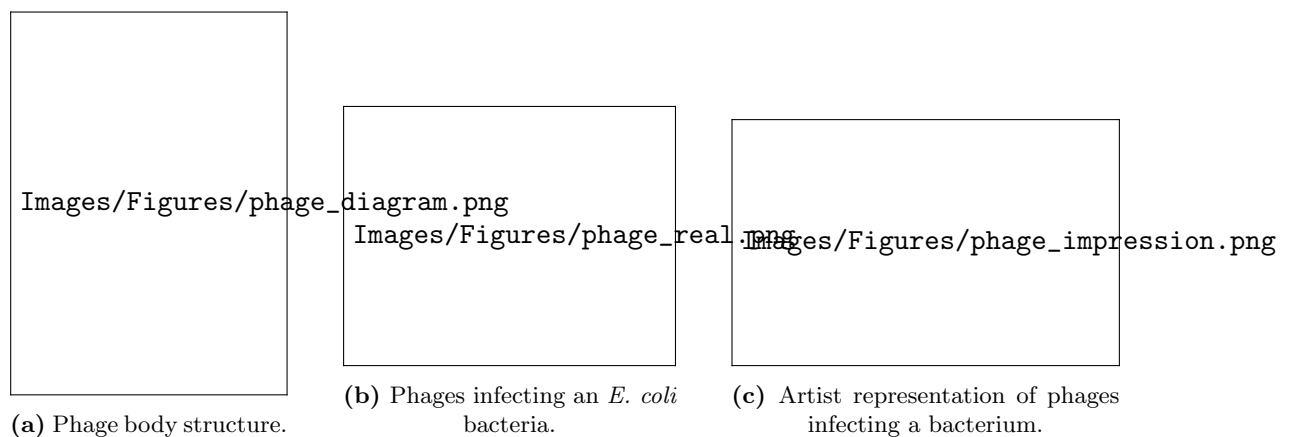


Figure 2.2: Parts of a phage, a real life picture of phages infecting an *E. coli* bacterium, and an artist's impression of phages infecting a bacterium.

2.2.2 How Does the Phage Cycle Work?

There are 3 main parts to the phage-bacteria host cycle, the infection stage, the lysogenic cycle, and the lytic cycle. Figure 1.1 shows a detailed overview of the phage cycle.

In the infection stage, a phage attaches to the surface of a bacteria cell. The infection stage involves the phage searching for, detecting, and attaching to a bacterium, followed by DNA injection. Detection and attachment occur via phage receptor-binding proteins located at the tip of the phage tail that recognize specific receptors on the bacterial cell wall, triggering conformational changes that enable DNA injection. The success of this process depends on the specificity and density of both phage and bacterial receptors [19]. Once attached, the phage injects its DNA into the host cytoplasm, where it can replicate independently. Once injected, the phage-cell pair can go into the lysogenic cycle or into the lytic cycle.

The lysogenic cycle involves phage DNA integrating into the bacterial genome as a prophage, where it is replicated along with the host cell without causing immediate lysis. The phage evades host defenses such as CBASS and CRISPR-Cas systems, which can start programmed cell death preventing phage replication or detect and degrade foreign DNA [20, 21]. Programmed cell death helps recycle resources for other bacteria [22]. Once integrated, the prophage can alter host fitness and provide resistance to other phages. During cell division, the prophage is copied into daughter cells but remains at risk of being excised by restriction enzymes [23]. Under certain stress conditions, such as DNA damage or activation of the SOS response, the prophage can be induced to exit the genome and enter the lytic cycle [19, 24, 25].

The lytic cycle is the process where a phage infects a bacterium, hijacks its replication machinery to produce new phage components, assembles these parts, and ultimately lyses the host cell to release new phages. This involves hijacking the host's DNA replication to synthesize phage parts like the capsid, sheath, and tail Figure 2.2a. The phage does this by redirecting resources from internal cellular functions towards viral replication [22]. The phage parts self-assemble via protein-protein and protein-nucleic acid interactions [26]. Phages induce bacterial lysis by producing holin proteins that disrupt the cell membrane, releasing the phages and resources [27].

2.3 Bacterial Defense Against Phages

There is a constant battle between phages and bacteria. The bacteria don't want to be killed by the phages, so they adapt defenses such as thickening of the cell wall or destroy the viral DNA.

2.3.1 Mutations in Bacterial DNA (Genetic (Co-)Evolution)

As bacteria cells grow and divide, random point mutations can occur in the DNA. These mutations can affect phage defenses, like thickening the cell wall or removing a receptor, making it harder for the phages to detect and infect the cell. Mutations can be partially effective if full effectiveness requires multiple steps to achieve. Random mutations can also fail at making the bacteria more resistant to phages by increasing phage susceptibility or the mutation brings a cost to the bacteria cell by losing receptors on the cell wall [28].

2.3.2 Horizontally Transferring DNA

Bacteria can horizontally transfer DNA to other bacteria on contact. A donor cell can donate DNA fragments using a mechanism called a pilus. The pilus acts as a tunnel between the donor cell and the recipient cell so that DNA can be transferred from the donor cell to the receiver cell [29].

A phage can accidentally collect a piece of the host's DNA instead of its own DNA during assembly. The phage with the now dead hosts DNA can infect the next bacteria, injecting the new bacterium with the dead cell's DNA, horizontally transferring the DNA [30, 31]. The transferred DNA can include natural phage defenses or significantly alter the genes and phenotype of the bacterium that future phages can't detect it anymore.

2.3.3 Phage Inactivation and Decoys

Bacteria can further protect themselves by producing decoys that the phage will attach to instead of themselves. Freshly lysed bacteria may still have biomarkers that attract phages, leading phages to attach to non-viable cells where successful infection cannot occur. Bacteria can also produce proteolytic enzymes that will damage the proteins found in a phage [32]. Some bacteria can produce outer membrane vesicles that phages can absorb to, and later detach and float away with the phage [33]. It is suspected that the impact of these vesicles acting as a sink is minor [34].

2.3.4 Phenotype Resistance

Not all new phenotypes arise from genetic mutations. Resistance can result from phenotypic variation within a genetically identical population, allowing bacteria to express different resistance traits without altering their DNA. Gupta et al. [35] found that some *Bacteroides fragilis* bacteria were able to evade phage infection. The presence of combinatorial phenotypic states where differential expression of protective mechanisms created rare super-resistant cells capable of withstanding phage attack. By acting together, these heterogeneously expressed anti-phage defense mechanisms created a phenotypic landscape where distinct protective combinations enabled the survival and re-growth of bacteria expressing these phenotypes without acquiring additional mutations.

2.3.5 Spatial Refuge/Biofilms

Usually bacteria and phages coexist in well mixed environments such as the ocean, however some environments offer natural structures for bacteria to hide behind. These

structures can range from physical structure, like sediment in water to biochemical structures like biofilms, where the phages can't diffuse through the biofilm. In large enough quantities, bacteria and other microbial communities create biofilms, a layer of mucus containing various microbes. The thick mucus, microbes, and other spatial effects help protect the bacteria in the biofilm from external phages by making it hard for the phages to penetrate and diffuse through the mucus [36]. In the case of a lab experiment on an agar plate, bacteria protect one another by making it harder for the phages to diffuse through the system [37].

Phage movement is passive, relying on diffusion through the environment or via pressure and temperature gradients [38]. Unlike phages, bacteria possess motility, allowing them to actively move through their environment increasing their chance of survival.

2.4 Phage Counter Defense Against Bacteria

With some of the defenses that bacteria have developed, phages are always mutating to counter their defenses. If phages don't adapt to the ever-changing bacterial defenses, the phages will die out due to their inability to infect and multiply. It essentially becomes an arms race, seeing who can out-adapt the other. A delicate balance therefore needs to be achieved so that both the bacteria and the phages can coexist.

2.4.1 Genetic Mutations

Mutations in viral DNA will affect how the phage body parts are designed and built. These mutations will affect external phage behavior such as how it detects a bacterium, as well as internal behavior such as evading detection and integrating with the cell's DNA. The changes will lead to changes in overall phage fitness, ie the ability for the phage to infect, replicate, and lyse bacteria.

2.4.2 Viral Recombination

Multiple phages can infect a cell and replicate itself using the cells internal replication process. Each phage has its own building blocks. If the proteins that build the subparts of each phage have similar chemical properties, they can be swapped between phages [26]. This allows for biological diversity to spread throughout a phage population. Each phage body part can have unique characteristics such as better attachment rate, larger DNA storage capsule, or better probability of injection.

2.5 Phage Defense Against Phages

Some phages can employ defenses against other phages from infecting the bacterial cell ensuring the host resources are all for itself. The act of preventing a secondary infection from a similar or closely related phage is called superinfection exclusion (SIE) [39]. There are various methods of preventing further infections that are listed below.

2.5.1 Altering Cell Structure

The prophage can alter the surface receptors of the bacteria, making it harder for other phages to detect the bacteria, reducing the chance of attachment and injection by other phages [40].

2.5.2 Protein Creation

Other phages like the T4 phage can create proteins like the Spackle protein which inhibits the lysozyme activity used in the process of DNA injection by other phages [40, 41]. Some prophages can encode proteins that will interfere with the replication process of other phages. For example, the SieA protein encoded by phage P22 blocks infection from other phages [42].

Tail Assembly Blocker (TAB) is an anti-phage defense mechanism encoded by a *Pseudomonas aeruginosa* prophage. While TAB permits the invading phage to replicate its genome, it inhibits the assembly of the phage tail, thereby preventing the production of infectious virions. The prophage that encodes TAB is not affected by this inhibition, as it also expresses a protein that neutralizes TAB's blocking activity. Although the host cell still undergoes lysis, no infectious phages are released.

2.5.3 Growth Curves Typically Seen in a Lab

When choosing parameter values it is important to choose parameter values that could realistically be found in real life systems and be replicated in the lab. There are various features that a researcher will be looking for in growth curve produced in a lab. A combination of these features results in an ideal growth curve that replicates real life bacterial growth.

The idealized dynamics of bacterial populations undergoing phage infection have several phases. First, there is a clear exponential rise in bacteria growth, and can expect to grow

40-100x in the span of a few hours. At a certain point in time, the bacteria population start decreasing, almost as fast as they were growing.

Phage populations also exhibit exponential growth, but with a delay in growth. There is initially no growth in phage population. After a set amount of time, the phage population will start to grow and peak a few hours after the bacteria population reached its peak. If there is no phage death or removal, the phage population will eventually reach a plateau when every bacteria has died.

Figure 2.3a shows an example of a curve for a $1 \times 1 \times 1$ system that would typically be seen in a lab. Figure 2.3b is the same plot but with a logarithmic y-axis. These specific plots exhibiting a clear growth, peak, delay, and death cycle.

Images/Plots/Created/a_good_curve_linear.png

(a) An example linear y-axis for a curve that researchers aim to replicate.

Images/Plots/Created/a_good_curve_logarithmic.png

(b) The equivalent logarithmic y-axis plot for a curve that researchers aim to replicate.

Figure 2.3: Growth population of a $1 \times 1 \times 1$ system. The log plot allows to see behavior happening at values approaching and to plot data on a logarithmic scale. The parameters used for this plot can be found in Table E.1.

2.6 Bacteria and Phages in the Lab

Researchers around the world are running lab experiments to gain further knowledge of the interactions between phages and bacteria. The aim is to better understand how phages work and interact with bacteria at a molecular, host, and population level.

2.6.1 Running Experiments

A researcher might run the experiment in a liquid medium containing water, carbon and nitrogen sources, and other chemicals such as anti-foaming or pH control chemicals. This liquid medium, often referred to as broth, allows for the cultivation of bacteria in a well-mixed environment, enabling researchers to monitor bacterial growth and phage infection dynamics over time. By adjusting parameters such as resource concentration, temperature, agitation speed, and pH, researchers can simulate different environmental conditions and observe their effects on phage-bacteria interactions.

Samples can be taken at various time points to measure bacterial density, phage titer, and resource concentration, providing quantitative data for model validation and hypothesis testing. The researcher received an ODE-like curve of the bacteria density. Researchers can create a mathematical interpretation of the bacteria growth curve and run curve fitting algorithms to find the bacteria's growth rate. The phage parameters such as latent time and burst size can be found by analyzing the phage one-step growth curve [1, 43].

2.6.2 Chemostats

Commonly used setups include liquids containing phages, bacteria, and resources in a chemostat and batch culture. Chemostats allow for continuous addition of resources and removal of waste, maintaining steady-state conditions ideal for studying long-term dynamics.

2.6.3 Petri Dishes

Petri dishes are another commonly used way to grow bacterial colonies. Agar, a jelly-like substance derived from seaweed, is commonly used as a solid growth medium in petri dishes. Agar provides a stable surface for bacteria to grow on and form visible colonies. When phages are introduced, clear zones called plaques appear where phages have infected and lysed the bacteria, allowing for quantification and observation of phage activity. The phages can diffuse on the agar plate, infecting neighboring cells. Phage infection creates clear plaques (2-3 mm) where bacteria are absent. Figure 2.4 shows an example of a bacteria lawn with phage plaques.

2.6.4 Measuring Growth

Bacteria density in clear liquid mediums can be measured optically using light. As the bacteria grow and die, the solution will get more cloudy. By shining a light through a vial with bacteria growth, the change in light refraction and intensity can be measured. A researcher might also be interested in using a mass spectrometer to measure the density of phages and resources at specific time points.

With petri dishes, it is harder to measure the bacterial growth. It might be possible to wash the bacteria off into a test tube with water to measure the optical density (OD), but the results are inconsistent. Even though using a special spectrophotometer allows consistent results, the results are dependent on the medium, the length of travel through the medium, bacteria size, and density. The device also has to be calibrated to ensure proper results, and results cant be compared across devices without calibration [44]. Changing methods to using $\frac{\text{cells}}{\text{ml}}$ instead of OD can be used to directly compare results across experiments, labs, and bacteria colonies [45].

It might be possible to quantify the change in plaque size, either by hand or using an image analysis program, but the results might be inaccurate and sensitive to different lighting conditions.



Figure 2.4: Bacteria lawn, the dots on the petri dish show no bacteria growth due to the presence of phages. Photo courtesy of S. Flickinger.

2.6.5 Serial Transfer

Serial transfer (ST) is a method employed by bacteriologist where after a set amount of time, the bacteriologist pipettes medium containing phages, bacteria, and resources out

of a test tube and adds the old media into a new test tube with new media. At this stage, the bacteriologist can add more bacteria or phages to the test tube. However, usually only resources are added during the transfer process. Researchers can optically measure the bacteria density using an optical density machine or employ a mass spectrometer to determine the phage concentration at set time points during the experiment. As the bacteria grow, they consume the resources found in the medium. The resources will eventually run out, and the bacteria die out due to a lack of resources. By introducing new resources at set time intervals, the bacteria can regrow and exhibit a semi-stationary behavior.

2.7 Software Mathematically Modelling Phages, Bacteria, and Resources

Some software programs modelling phage-bacteria-resource interactions already exists.

2.7.1 Cocktail

Nilsson [4] developed Cocktail to model phage-bacteria-resource kinetics in a chemostat. The model assumes there is one bacteria strain that can be infected by phage A and phage B, and by both phages at the same time, phage AB. The model models bacterial resistance to phage A, B, and AB. The user can control the parameter values such as resistance rate to A, B, and AB, resource concentration and outflow, and phage adsorption rate. The user can also control model settings, such as if the model is deterministic or stochastic, and the step size [4]. Four sample output plots are shown in Figure 2.5a.

2.7.2 PhageDyn

PhageDyn is a Java applet that models phage dynamics in multi-reactor industrial wastewater treatment plant models. PhageDyn interacts with existing GPS-X [46] files to incorporate phage dynamics into models of industrial wastewater treatment plants [5]. Krysiak-Baltyn et al. [5] developed PhageDyn to determine how phages can reduce foaming caused by bacteria in wastewater treatment plants, another real life application of phages [47]. PhageDyn does not simulate phage dynamics on its own but rather manipulates existing files in GPS-X in order to incorporate phage dynamics in wastewater treatment plant models. Figure 2.5b shows the output that PhageDyn provides.

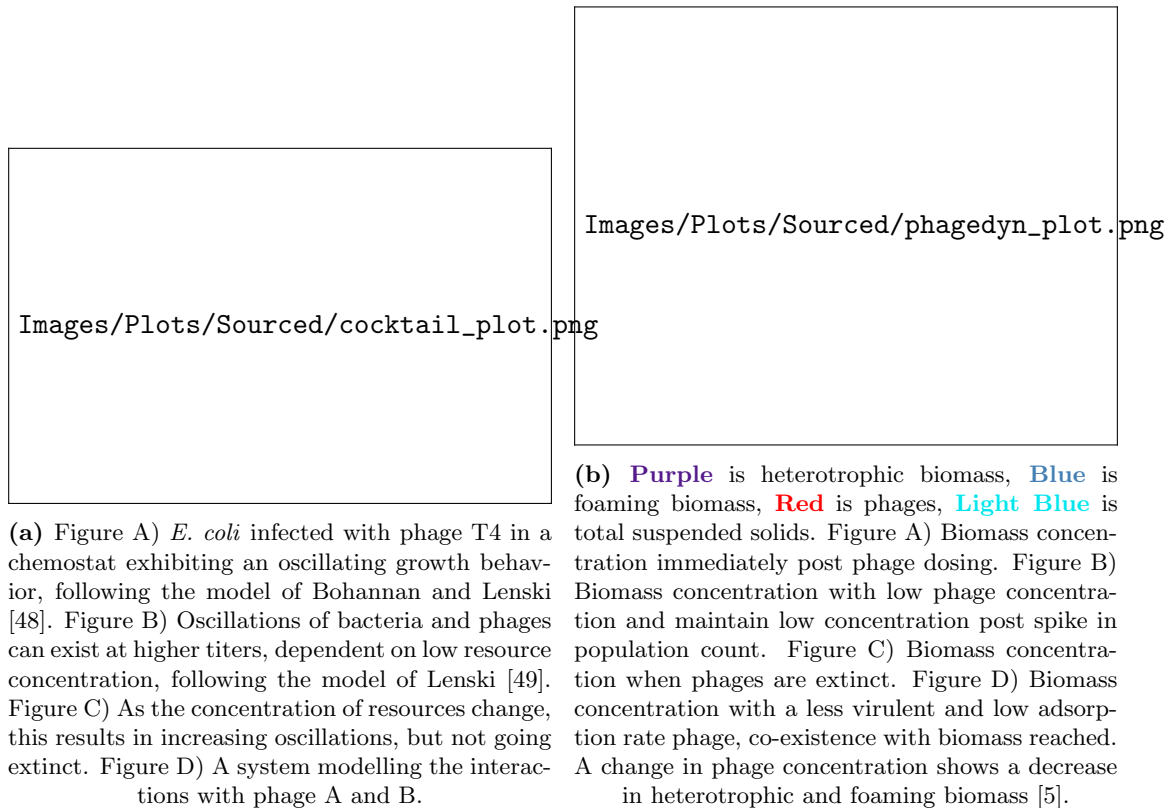


Figure 2.5: Example output from Cocktail and PhageDyn respectively. For PhageDyn, concentration of heterotrophic biomass in an aerobic plug flow across four situations. See Nilsson [4] and Krysiak-Baltyn et al. [5] for more information on parameter values and supplementary resources.

2.7.3 Cocktail and PhageDyn Limitations

There are limitations to Cocktail and PhageDyn. Cocktail can model up to a $2 \times 1 \times 1$ system, and is designed to model a chemostat. Chemostats receive a constant influx of new resources and a constant removal of medium from the chemostat. Cocktail's model can not be easily adapted to other models. The ODE model accepts inputs from a hardcoded GUI frontend. So any changes to the frontend or to the ODE model will require changes to the ODE model and the frontend to accept the new inputs and outputs. The code for Cocktail is open source, so adding new buttons and changing the model should not pose a significant challenge, but still an undertaking.

PhageDyn works with GPS-X, a very niche wastewater treatment modelling software. PhageDyn is programmed for a very specific task with no flexibility in changing the model or inputs. PhageDyn assumes biomass, instead of individual bacteria populations. However, PhageDyn is no longer available for download.

2.8 The Golding Model

The default model that will be used in this thesis, the “Golding model“, sourced from Geng et al. [1], describes the interactions between resources, uninfected bacteria, infected bacteria, and phages.

2.8.1 The Original Golding Model

The model describes three biological processes, cell consumption of resources and growing, phage/cell encounters and infection, and cell lysis. The cell growth process is described by $g(R, v, K)$, the instantaneous growth rate dependent on the Monod equation, where v is the maximal growth rate of the bacteria population and K is the Monod constant. Bacteria consume a resource with rate e .

Once infected by a phage, the bacteria goes from U to I_1 . The bacteria goes through M stages of infection I_1, \dots, I_M before lysing, The bacteria goes from state I_k to state I_{k+1} with equal transition rate $\frac{M}{\tau}$. The infection rate of a cell is r . After a bacteria lyses after stage I_M , β phages are released, the burst size of the phage.

Equation 2.8 The Golding model sourced from Geng et al. [1]. The text in **red** has been added to the model, adding (the wash-in) fresh resources (ω^i) and the removal (wash-out) of entities (ω^o). The washin is not dependent on the current resource population, as it is a constant rate being added. By default these values are 0. A summary of the parameters can be found at Table A.1.

$$\frac{dR}{dt} = -e \cdot g(R, v, K) \cdot (U + \sum_{k=1}^M I_k) \quad (2.3)$$

$$\frac{dU}{dt} = g(R, v, K) \cdot U - r \cdot U \cdot P \quad (2.4)$$

$$\frac{dI_1}{dt} = r \cdot U \cdot P - \frac{M}{\tau} \cdot I_1 \quad (2.5)$$

$$\frac{dI_k}{dt} = \frac{M}{\tau} (I_{k-1} - I_k) \text{ for } k = 2, \dots, M \quad (2.6)$$

$$\frac{dP}{dt} = \beta \cdot \frac{M}{\tau} \cdot I_M - r \cdot (U + \sum_{k=1}^M I_k) \cdot P \quad (2.7)$$

$$g(R, v, K) = \frac{v \cdot R}{R + K} \quad (2.8)$$

2.8.2 The Adapted Golding Model

The original Golding model is specifically designed for a $1 \times 1 \times 1$ system. In order to adapt this model to fit an $p \times b \times r$ model, the model needs to be slightly adapted. There are other changes that can be made to the model, for example by adding a washin rate ω^i , where resources are constantly being introduced, and a washout rate ω^o where all entities are washed out at a constant rate. These changes are highlighted in Equation (2.14) in red.

The adapted model accounts for the interactions of multiple phages, bacteria, and resources, and assumes the interactions occur independently of one another.

Equation 2.14 The adapted Golding model. The probability of phage p infecting bacteria b is r_{pb} is not to be confused with the resource concentration R_r . The interactions are a sum of all interactions due to all interactions taking place at the same time.

$$\frac{dR_r}{dt} = - \sum_{b \in B} e_{br} \cdot g(R_r, v_{br}, K_{br}) \cdot (U_b + \sum_{k=1}^M I_{b_k}) + w^i - w^o \cdot R_r \quad (2.9)$$

$$\frac{dU_b}{dt} = U_b \cdot \sum_{r \in R} g(R_r, v_{br}, K_{br}) - U_b \cdot \sum_{p \in P} r_{pb} \cdot P_p - w^o \cdot U_b \quad (2.10)$$

$$\frac{dI_{b_1}}{dt} = U_b \cdot \sum_{p \in P} r_{pb} \cdot P_p - \frac{M}{\tau_b} \cdot I_{b_1} - w^o \cdot I_{b_1} \quad (2.11)$$

$$\frac{dI_{b_k}}{dt} = \frac{M}{\tau_b} (I_{b_{k-1}} - I_{b_k}) - w^o \cdot I_{b_k} \text{ for } k = 2, \dots, M \quad (2.12)$$

$$\frac{dP_p}{dt} = \sum_{b \in B} \beta_{pb} \cdot \frac{M}{\tau_b} \cdot I_{b_M} - r_{pb} \cdot (U_b + \sum_{k=1}^M I_{b_k}) \cdot P_p - w^o \cdot P_p \quad (2.13)$$

$$g(R_r, v_{br}, K_{br}) = \frac{v_{br} \cdot R_r}{R_r + K_{br}} \quad (2.14)$$

Chapter 3

Methods

3.1 Project Overview

To help complete this Master thesis, I created various tools that would help create the final model outputs. The project is divided into four parts.

- Using a GUI network creation tool to define the number of phages, bacteria and resources in the network, and their interactions.
- The simulation framework handles the data, runs the ODE simulations, and sends the data back to the dashboard.
- A dashboard that the user can interact with to run simulations, edit parameter values, and plot and interact with the visualizations.
- Download the data to create your own custom visualizations and analyses.

A flowchart showing the user-system interactions can be seen in Appendix C.

3.1.1 Network Creation Tool

The user uses the GUI network creation tool to create and edit the network interactions. There are three types of variables in the simulations: phages, bacteria, and resources. Every node in the network represents either a phage, bacteria, or resource. The bacteria can be further divided into uninfected and infected bacteria. An edge links two nodes together if there is an arbitrary interaction occurring between them. Bacteria are infected by phages and take up resource. Which phage can infect which bacteria and which resources each species of bacteria can take up describes a network of interactions.

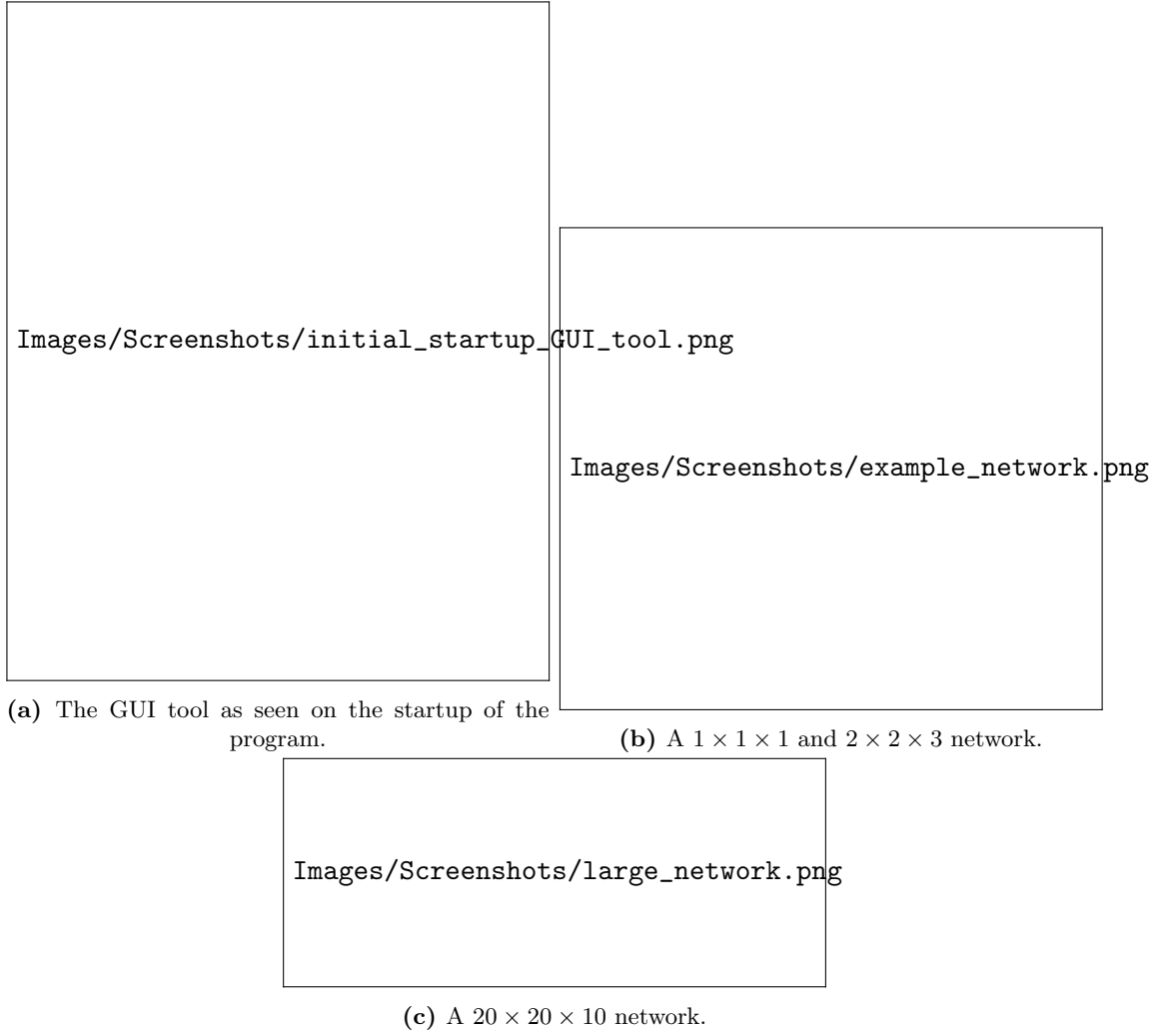


Figure 3.1: This network topography along with a $1 \times 1 \times 1$ network will be used in the Chapter 3 and Chapter 4 sections. The parameter values for the networks can be found at Table E.1, Table E.4 and Table E.3 Each node represents a phage, bacteria, or resource, with arbitrary interactions occurring between them. Although not shown and used here, edges between the same entity types and self loops are allowed.

Finally, the user can export (and later import to edit) the network representation for use in Section 3.1.2, Section 3.1.3, and Section 3.1.4. Figure 3.1 shows the layout of the GUI tool and example networks that can be created.

3.1.2 Simulation Framework

The user provides an ODE model and the network topography as input to the framework. The simulation framework deals with handling the input, output, collecting and storing of the simulation input and output. The framework uses SciPy's [50] `solve_ivp()` numerical solver [51] to simulate the provided ODE equations and calculate the population levels through time. The user receives two outputs from the framework. The first

output is an array of time values that the solver used to calculate the population count. The second output is an array containing the population count at each time step for every entity.

In order to facilitate more complex model behavior, extra entities can be added to the simulation. Such an example would be the distinction between uninfected and infected bacteria. In the network model you explicitly create a $3 \times 2 \times 3$ network, with 3 phages, 2 bacteria, and 3 resources. You explicitly tell the solver to add $2 \cdot M$ additional states that represent the infected states. So the ODE solver would solve for 3 phages, 2 uninfected bacteria states, $2 \cdot M = 2 \cdot 4 = 8$ infected bacteria states, and 3 resources.

Adding a resource reservoir to the model would be simple as well. 3 extra resource entities would be added to the system, where the resources would model the transfer of resources from the reservoir to the simulation environment. The provided ODE model will have to correctly model and transfer the resources from $R_{r_{\text{reservoir}}}$ to $R_{r_{\text{chemostat}}}$. The bacteria would only consume from $R_{r_{\text{chemostat}}}$.

The user's ODE model has to correctly model each (extra) entity and correctly handle the changes in states.

3.1.3 Visualization Dashboard

The third part involves analyzing and visualizing the simulation results on an interactive Dash Plotly [52] dashboard. The user can use a dashboard built using Plotly Dash to interact with the solver and network. The user can quickly change parameter, environment, and setting values with the dashboard. As output, the dashboard will show interactive plots so that the user can analyze the system.

The dashboard allows the user to interact with the network, the model, and some prebuilt visualizations, and is built into three logical sections. The first section allows for the user to edit the network parameters and setting values on the fly to quickly iterate through different conditions and to fine-tune parameter selection without having to rebuild the network using the GUI tool. The second section allows for the user to see how the population count evolves over time for a given IC and parameter values, allowing to quickly test the network input. The final section allows for the user to run more advanced analyses on the network, for example, by changing multiple parameter values and visualizing the output.

3.1.3.1 Editing Network and Parameter Values

The editing network and parameter value contain five separate sections.

Initial Condition The IC settings panel (Figure 3.2a) allows the user to edit the initial starting values of the entities. Each entity type has a table containing the initial population count.

Vector Data Data that can be represented as a vector have their own section. This data would typically be seen with node data. So the washin rate of resources, or how fast a bacteria goes through the infection stage would be represented as a vector Figure 3.2c.

Matrix Data Data that is stored as a matrix, the data stored on edges between entities, is stored in the matrix tab, Figure 3.2b. This would typically be data that is stored on the edges, for example the phage infection speed or how fast a bacteria can consume a resource.

Environment and settings The environment data and settings data also have their own tab, Figure 3.2d and Figure 3.2e respectively. The data stored in the environment act as global variables, like the pH of the system, or the constant washout rate. The settings node holds the solver and simulation settings like the length of the simulation or minimum time-step.

3.1.3.2 Visualization and Analysis

In the analysis section, the user can run different analysis methods to gain a greater understanding of the model. For simplicity, the visualizations on the dashboard only support a $1 \times 1 \times 1$ model. This makes it easier for the user to analyze the system. The goal of the dashboard is to investigate a simple system in order to gain a deeper understanding of the system. There are five prebuilt visualizations which are described below. These five visualizations are called serial transfer, parameter analysis, initial value analysis, serial transfer, and SOBOL analysis. The aim of the visualizations is to investigate how the system changes with respect to varying inputs.

After the user has a deeper understanding of the system, they can run and download custom simulations to create their own custom visualizations in the Ultimate Analysis section. The saved simulation data is stored as a *.parquet* file, a tabular-like data format.



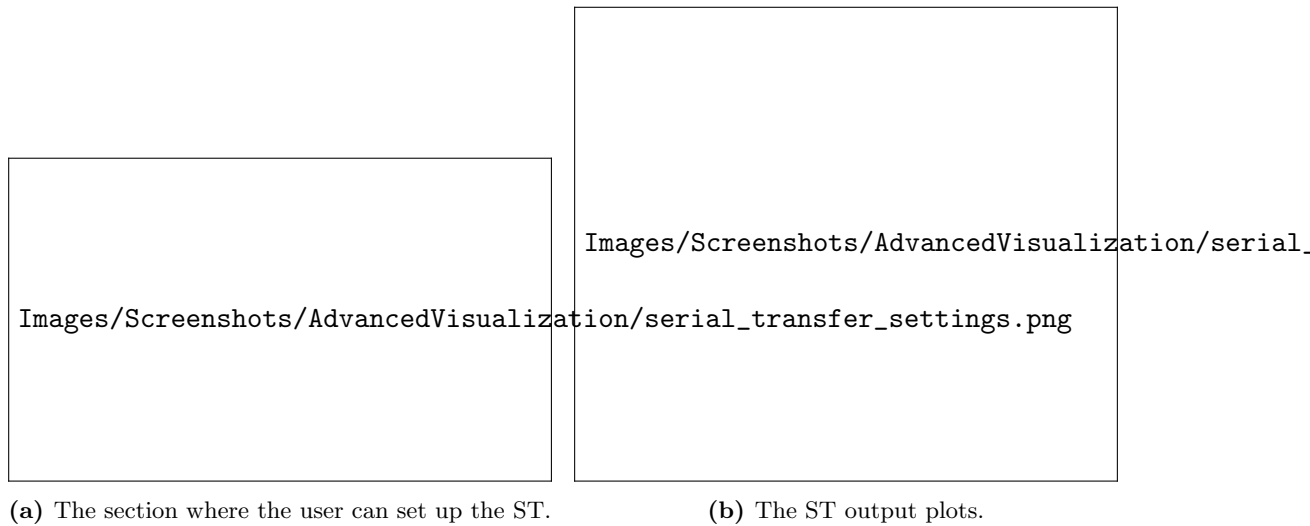
Figure 3.2: The tabs where the user can edit the various parameter values and control the simulation parameters

The simulation data can be queried with Dask, allowing a user to find a specific simulation result. Parquet with Dask offers superior performance and data storage solutions that Pandas doesn't offer.

Serial Transfer On the dashboard, a user can select the dilution factor which will divide the population count of the phages, bacteria, and resources by that number (Figure 3.3a). Then the program takes the IC values defined in Section 3.1.3.1 and adds those values to the respective entity.

As an example, if the simulation ended with 3500 phages, 100 (uninfected) bacteria and 50 resources, the dilution factor is 10, and the user wants to add 350 new bacteria and 130 new resources for the next simulation, the new starting condition for the next simulation would be $\frac{3500}{10} = 350$ phages, $\frac{100}{10} + 350 = 660$ bacteria, and $\frac{50}{10} + 130 = 135$ resources.

As output, ST will show how the population evolved through time as well as the final population value at the end of each serial transfer run. An example output is shown in Figure 3.3b.



(a) The section where the user can set up the ST.

(b) The ST output plots.

Figure 3.3: Serial Transfer

Parameter Analysis The parameter analysis (PA) settings tab as shown in Figure 3.4a allows the user to choose two parameters and individually run the model with the varying input values. The values that can be tested and changed include all IC values, vector and matrix data, and environmental data. As input, the user can select 2 parameters of choice. After the parameter name selection, the user can manually choose which parameter values they want to test or test a range of values equally spaced by selecting the number of values to test. Finally, the user can optionally run a ST, where the ST uses the settings found on the ST tab.

Figure 3.4b shows the heatmap that the user can expect, one heatmap for each entity type. Each heatmap cell represents the input of 2 unique parameter values, and shows the population count for that parameter run at the time shown in the slider. As the user

slides the slider, the value inside the cell updates to correspond with the selected time. Note that the heatmap color range resets for each heatmap, so similar colors across heatmaps and across time will not correspond to the same values.

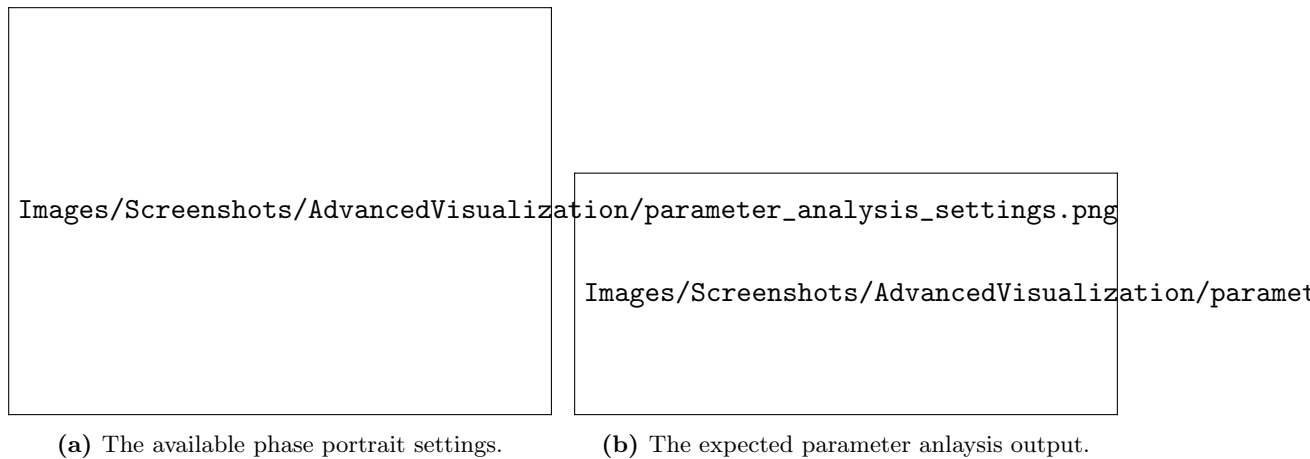


Figure 3.4: Parameter Analysis

Initial Value Analysis The initial value analysis (IVA) settings tab as shown in Figure 3.5a allows the user to choose a single parameter and vary the value of that parameter, visualizing how a change in parameter value affects the population count of the entities.

Figure 3.5b shows the plots that the user receives. For each entity type, there are three plots made. The left plot shows the population count through time, one line for each parameter value submitted. The middle plot takes each run and calculates the “percentage from the max value” (default value of 0.95 \rightarrow 95%) reached of the peak. This value is considered the time of peak, and is used to fix some issues that can arise where the population plateaus or only keeps on rising. The initial value is plotted on the x-axis, with the time at which the max value is reached on the y-axis. Using the plotted data, a linear or log fit can be created. In Figure 1 of Mulla et al. [43], they vary the initial bacteria concentration and measure the time until bacterial collapse. The initial concentration and corresponding collapse time are plotted on logarithmic x and y axes, with a linear regression fitted to the log-transformed data. The observed logarithmic decrease suggests that the phage kinetics is adsorption-limited. Figure 4.2a replicates this graph.

Using the IVA tool can be useful for understanding how a change in parameter value affects the time at which the population count reaches a maximum. The slope, intercept and R^2 value is stored and saved in the third plot, a bar chart, with an editable name. For every re-run of the IVA, the slope, intercept and R^2 value is stored in the bar chart.

When executed with multiple parameters, this enables comparison of high-level results across various parameters and experimental conditions.

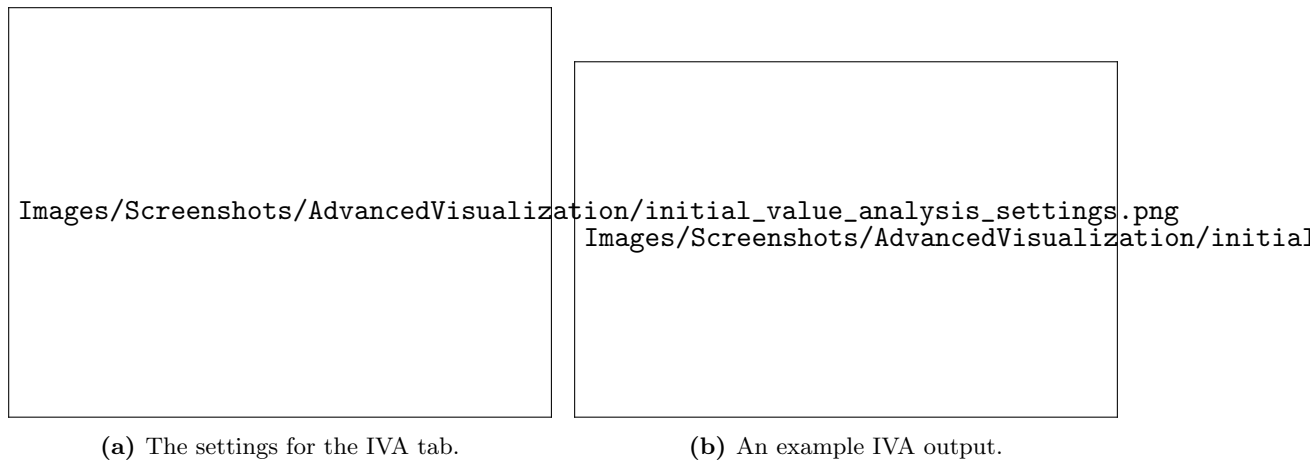


Figure 3.5: The IVA settings and output.

Phase Portrait The phase portrait plot allows the user to analyze how an entity population evolves with respect to the other entity population through time. Phase portraits indicate how one population increases while the other decreases, and vice versa. Steady states can be identified and classified as either stable, unstable, or as saddle points. It is also possible to visually identify attractor and repeller points by seeing where the population values trend towards. By comparing different starting points, it is possible to see if the system is chaotic or not. The setup for the phase portrait can be seen in Figure 3.6a, and a sample output can be seen in Figure 3.6b.

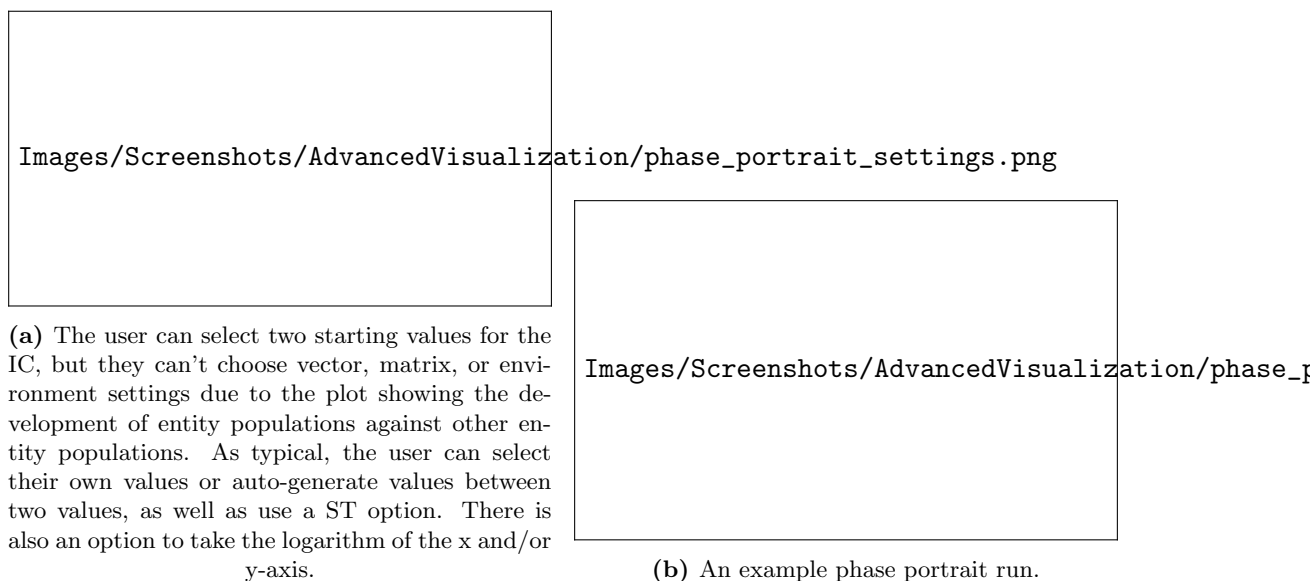


Figure 3.6: Phase portrait settings and output.

SOBOL Sensitivity Analysis It is important to understand how a change in parameter value affects the change in output of a model. Models will have parameters that are more important and have a larger effect on the model output than other parameters.

SOBOL analysis [53], a variance-based sensitivity analysis, is a method that allows a user to quantify how important an input parameter has on a measured aspect of the output by changing the input parameter values of the model and measuring the change in model output. SOBOL can only measure a single univariate model output, for example the final population value, smallest or largest value reached, the time at which the largest value was reached, or any other univariate output. SOBOL quantifies how much variance in the output can be attributed to a specific parameter and can measure the effect of global/total (ST), first ($S1$), and second order sensitivity ($S2$).

First order Si , or local sensitivity, is the measurement of the effect that parameter i has on the variance of the output. Second order is the measurement of parameter i interacting with parameter j , and how the interaction attributes to the output variance. Etc for third order and higher. Global, also called total sensitivity, is the summation of all interactions. If $ST_i \gg S1_i$, then parameter i depends on higher order interactions with other parameters, while when $ST_i \approx S1_i$, then i doesn't interact much with and depend on other parameters. It should be stated that $ST_i \geq S1_i$ and that ST_i can be greater than 1, while $S1_i \leq 1$.

When a model is viewed as a black-box model, the model can be seen as a function $Y = f(X)$, where X are the parameter values of d elements, and Y is a univariate model output. X is assumed to be independently and uniformly distributed within a hypercube $X_i \in [0, 1]$ for $i = 1, \dots, d$. The first order sensitivity measures the output variance of the main affect of parameter X_i . Measuring the effect of varying X_i averaged over other input parameters, and standardized to provide a fractional contribution to the overall output variance. The first order sensitivity is described as

$$S1_i = \frac{V_i}{Var(Y)}$$

where $V_i = Var_{X_i}(\mathbb{E}_{X_{\sim i}}[Y|X_i])$ and where $X_{\sim i}$ represents all the parameters that are not X_i . All parameters are summarized in Table A.2

The second order index measures the impact of input X_i interacting with X_j . For many inputs, this becomes unwieldy to analyze. The global sensitivity is used to analyze the global sensitivity without evaluating $2^d - 1$ indices, and measures the contribution to the output variance of X_i , including all variance due to X_i 's interaction with other variables.

$$S1_i = \frac{\mathbb{E}_{X_{\sim i}}[Var_{X_i}(Y|X_{\sim i})]}{Var(Y)} = 1 - \frac{Var_{X_i}(\mathbb{E}_{X_i}[Y|X_{\sim i}])}{Var(Y)}$$

SOBOL accepts a list of parameter names and a list of range of values to sample from, which the user can input in the SOBOL settings tab, Figure 3.7a. If no values are added, the parameter is not included in the simulation and the default value is instead used. The user then needs to select the number of samples to run, using the formula 2^x , where x is the number they input, and 2^x is the number of samples that SOBOL will create and run. The larger x is, the more accurate the SOBOL analysis results will be, but the more simulations would need to be run. If 2nd order is not chosen, the model is run $N(D + 2)$ times. If the user wants to analyze the second order interactions, then the model will run the system $N(2D + 2)$ times with the randomly sampled input values, where N is a multiple of 2, and D is the number of parameters being tested. Due to the randomness of the sampling method, the user can, but does not need to, submit a seed value.

The global and first sensitivity are shown next to one another, and each sub-row within a plot represents each entity type. The proportion of the global and local sensitivity can be seen for each entity type and each parameter.

Upon completion of a SOBOL analysis, the original simulation data is saved to the disk as a *.pickle* file so that the user can reuse the data and run their own SOBOL analyses.

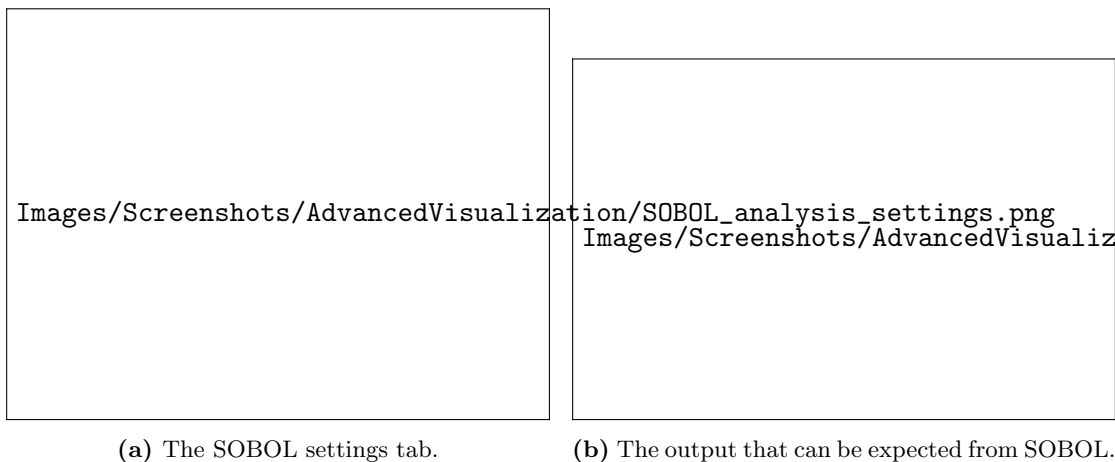


Figure 3.7: SOBOL variance analysis settings and output.

Ultimate Analysis Making a dashboard that can be used for different inputs is hard to make. Predicting the type of plots that a user might be interested in, and the type of behavior the user wants to analyze is impossible to predict. The Ultimate Analysis section does not produce any visualizations or analysis, but instead allows for the user to define which ICs and parameter values they want to run a simulation on. The solver will iterate over every single parameter input possibility and save the results in a *.parquet* file. Similarly settings in the other sections, the user can specify a start and end value, along with the number of values to generate evenly spaced within that range, including

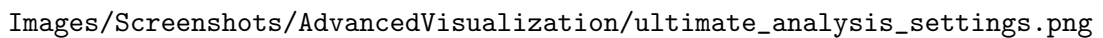
The image is a placeholder for a screenshot of the 'ultimate analysis setup tab'. It contains the text 'Images/Screenshots/AdvancedVisualization/ultimate_analysis_settings.png'.

Figure 3.8: The ultimate analysis setup tab.

both the start and end values (Figure 3.8).

Using Dask and the saved *.parquet* file, the user can query for specific runs, for example runs where a parameter value was greater than 0.05, and use the simulation data to create their own plots.

3.1.4 Custom Visualizations and Analyses

The final part, an optional step, allows the user to define a number of parameters they want to simulate and download the simulation results. The user can use this data to create their own custom visualizations without having to rerun the simulations, especially if there are many simulations. The data can be further processed and visualized as the user wishes.

As the dashboard can not create a graph for every situation, or be easily adapted to analyze every situation, Section 3.1.3.2 can be used to run and download the simulation data to the disk to later create your own custom visualizations.

3.2 Software Used and Packages

The program was created exclusively in Python [54], and makes extensive usages of various packages, ranging from the standard scientific packages such as NumPy [55] and SciPy to more niche packages such as pickle and SALib [56, 57].

The graphical tool uses Tkinter acting as the front end, handling the user inputs, while NetworkX [58] stores the graph and contains the attribute data of the edges and nodes. The GUI tool also uses Matplotlib [59] to create the figure of the graph to display to the user in the GUI tool.

The simulation framework, the backend of the modelling, makes extensive usage of SciPy's *solve_ivp()* to create the ODE data. It also makes light usage of NetworkX to load the graph and parameter values, as it initially takes a graph as an input. NumPy is used to set the parameters up at program startup.

The visualization part makes heavy usage of Dash and Plotly. Dash acts as the server and is used for displaying the HTML aspect of the frontend and dealing with any input and output. Upon choosing parameter values and clicking on “submit“, Dash registers the activity and calls the function registered to the button, sending data such as parameter values and options like “log x-axis” from the frontend to the backend server. In the backend, the various inputs are handled, like changing the input string “0.05, 0.1, 0.15, 0.2” into an iterable list $[0.05, 0.1, 0.15, 0.2]$ that the simulation framework can iterate over to vary the parameter value.

If there are many simulations to run through, in the case of Section 3.1.3.2, an intermediate call to a parallel computing library Joblib is called. Joblib parallelizes the computations on multiple CPUs to speed up computing time.

Ultimate analysis uses Pandas to write the data to a *.parquet* file. Pandas parquet offers efficient data compression, efficient memory usage and when combined with Dask, efficient querying functionalities in a Dataframe format that many data scientists would be familiar with.

SOBOL uses the SALib library to sample and analyze the parameter input. Both ultimate analysis and SOBOL save a *.pickle* file containing a dictionary with the parameter values tested, setting values, and other important information regarding the simulation.

Section 3.1.3.2 uses SciPy's *curve_fit()* function to curve fit the points in the middle plot (Figure 3.5b).

Other packages that are used include collections, copy, warnings, itertools, os, datetime, json, gc, and time.

Chapter 4

Experiments and Results

In the following section I will apply the software to demonstrate the predicted dynamics of the phages and bacteria under different conditions. I first begin with analyzing the model using a SOBOL analysis on the simple Golding model, Equation (2.8). Using the most important parameters identified from the SOBOL analysis, I run multiple IVAs to describe the change in graph behavior for different inputs. I use the information gained from this to describe how the graphs change for a wide range of inputs. Next, I analyze if phages will proliferate or not depending on the initial phage, uninfected bacteria, and resource concentration. I finally extend the analyses to a large community and analyze how changing parameter values will change the phage and bacteria growth, and if the phages and bacteria can coexist or not.

4.1 SOBOL Sensitivity Analysis Results

The SOBOL method is a global sensitivity analysis technique that quantifies the contribution of each input parameter, as well as their interactions, to the variance of a model's univariate output. It decomposes the output variance into fractions attributed to individual parameters and their combinations, providing first-order and total-order sensitivity indices. A SOBOL analysis identifies the most influential parameters affecting model output. The insights from this analysis inform the selection of key parameters for subsequent simulations, ensuring that further investigations focus on those with the greatest impact.

Figure 4.1a shows the impact that the parameter had on the final value of the population at $t = 15$ for a $1 \times 1 \times 1$ system, on the original Golding model, Equation (2.8). Figure 4.1b shows the impact that the parameter had on the peak population count, using the 95%

rule. Figure 4.1c shows the impact that the parameter had on the time of the peak, using the 95% rule.

The parameters that were tested include all the parameters listed in the basic Golding model, except for the uninfected bacteria (I_1, \dots, I_4) , M , ω^i , and ω^o . Infected bacteria was not included as it doesn't make sense to start with infected bacteria to the system. M , the number of stages that the infection goes through, can not be tested as SOBOL as M is an integer, while SOBOL randomly chooses float values. While testing, the washin rate ω^i and washout rate ω^o consistently had the largest influence on the final, peak value, and time of peak value, using the 95% rule. Washin and washout are not part of the original model from Golding, and the addition of a washin and washout term significantly skews the results and analysis, so it was left out of the analysis. The results for a SOBOL analysis with washin and washout can be found in Appendix F.1.

4.1.1 Resources

The final value for the resources depended heavily on the initial resource concentration. There weren't many interactions with other parameters because $ST \gg S1$. e had little influence on the system despite e acting as the link between the resources and bacteria and directly controlling the rate of resource consumption. τ had a larger influence in the final resource value than e .

The peak value and time of peak value graphs are empty for the SOBOL indices for Resources as the resource concentration is always decreasing from different initial conditions, the initial resource always had a peak at $t = 0$.

4.1.2 Phages

The final phage population value depended on r the most, with β as the second most important parameter influencing the final population value. The other parameters had little to no influence on the final phage population levels.

The SOBOL peak value plot is basically the same as the final population value. Similar to the final value, the phage max value is highly dependent on the value of r and β , and the other parameters had little to no influence on the peak value for the phages.

For the time of peak value, τ becomes the most important parameter for determining the time of peak value, while r isn't as important anymore. The initial phage population has a small influence on the final population value, about as equally important as r . β

roughly maintains the same sensitivity value across the final, peak, and time of peak analyses.

4.1.3 Total Bacteria

The final total bacteria population depended mostly on β , the burst size of the phage, but via many second or there are many higher order interactions occurring as $ST \gg S1$. The final population depended heavily on many higher order interactions with the initial resource concentration, τ , and e .

β is still the most important parameter to the model, but instead of ST and $S1$ being equal to 1 and 0.28 like in the final value, the sensitivity value is only 0.54 and 0.16 respectively. Every parameter plays some influence on the output, but with higher order interactions as for all parameter inputs, $ST > S1$.

β and τ are the two most important factors in determining the time of peak for the total bacteria. The only parameter that does not influence the time of peak in some manner is e , otherwise every parameter has some sort of influence on the time at which the bacteria population peaks.

4.1.4 Results

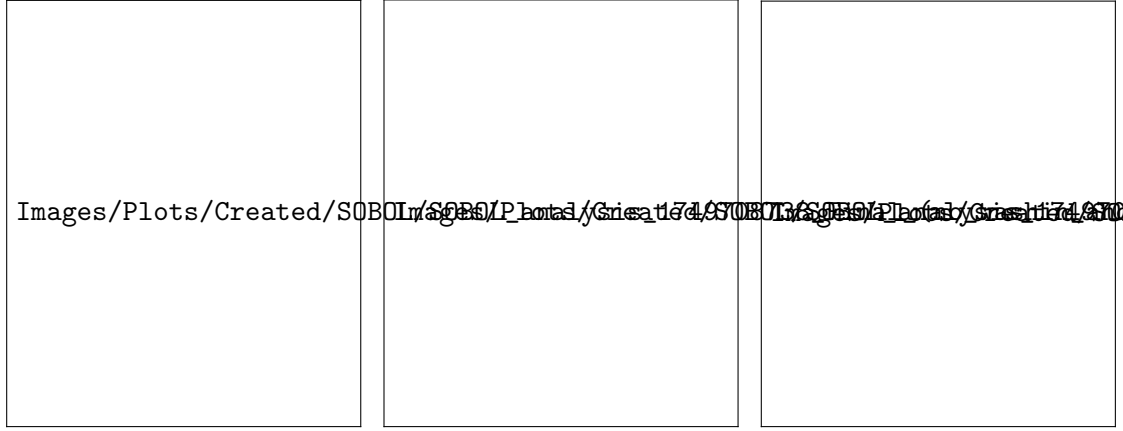
Some results are surprising. e , v , and K are consistently the least important factor in determining the final value, peak value, and time of peak. It would be expected that changing the parameter values that directly affect the bacterial growth would have a large impact on the resources and phages. More bacteria mean more resources are consumed, and more phages are created. Knowing that e , v , and K are relatively unimportant compared to a parameter like r or τ , future analyses do not have to focus on e , v , and K . As β , r , and τ are relatively important, future analyses could focus on how those parameters influence the growth of phages and bacteria.

4.2 Graph Behavior with IVA

Figure 2.3a is used as a “ground truth” for what a researcher would aim to replicate in a lab. Table 4.1 quantitatively elaborates how a change in parameter value across multiple values changes the shape of the population curves. Only the most important parameters identified in the SOBOL section, will be analyzed, so initial resource concentration, τ , r , and β .

Parameter	Tested Value	Behavior Description
R (400)	500	More uninfected and infected bacteria, slightly more phages. Resources last longer before being depleted.
	300	Slightly less uninfected and infected bacteria, slightly less phages, and earlier resource depletion.
U (50)	70	Slightly more phages and uninfected and infected bacteria. Resources are depleted faster.
	30	Less uninfected and infected bacteria, slower resource depletion, not all resources used, slightly less phages are created.
P (10)	20	Less resources consumed, less bacteria created, bacteria population peaks earlier, slightly less phages.
	5	Resources are consumed faster, more uninfected, infected, and phages. Bacteria population peaks at a later time.
τ (2.14)	3	Bacteria population peaks later, with a plateau in population after peaking before infections take place. Phages population is still growing. Infected bacteria peak significantly later. Significant increase in bacteria population.
	0.5	Barely any resource consumption, little bacteria growth and uninfected, more phages created, phages reach final value very fast. Bacteria population peaks very early.
ω^i (0)	15	Slightly more bacteria are created, resource replenish after bacteria die out. Resources are not depleted and regrow after bacteria die out. Slightly more bacteria are created.
e (0.03)	0.1	Faster resource depletion, sharper decline in uninfected, slightly less infected bacteria and phages. Drop in uninfected bacteria happens faster. Bacteria sum peak is sharper and happens earlier.
	0.01	Not all resources are consumed, slightly more bacteria are created.
v (1.2)	1.8	Resources are finished faster, significantly more uninfected and infected bacteria. Bacteria population peaks earlier, and there are more phages. Peak of the bacteria curve is more sharp and less rounded.
	1	Less phages and bacteria are created, not all resources are consumed, bacteria population peaks a tiny bit earlier.
K (10)	500	Not all resources are consumed, less bacteria and phages are created, earlier bacteria peak.
	1	Faster resource depletion and sudden stop instead of gradual slow-down, more uninfected, infected, and phages create.
r (0.01)	0.1 0.1	Less resource consumption, significantly less bacteria and phages, earlier peak in bacteria.
	0.001	Faster resource consumption rate, significantly more bacteria and phages, delay in uninfected and infected peak, sharp uninfected bacteria peak, sharp bacteria sum peak with a mini plateau before dropping.
β (20)	50	Significantly more phages and significantly less bacteria, earlier bacteria peak, less resources consumed. Steeper fall in uninfected bacteria, steeper rise in infected bacteria.
	10	Faster resource consumption, significantly more uninfected, less phages, sharper uninfected and total bacteria peak, total bacteria population has a plateau before falling.
ω^o (0)	0.02	Faster resource depletion, more bacteria created, later peak in bacteria population. Faster decrease in uninfected bacteria, slightly less phages created, with a gradual decrease in phages post peak.

Table 4.1: A table that compares how moving one individual parameter value up or down relative to Figure 2.3a changes the general shape of the curve. Reference parameter values used to compare the produced curves are included in the parentheses, taken from Table E.1.



(a) Final value, no washin and washout. (b) Peak population value, no washin and washout. (c) Time of peak value, no washin and washout.

Figure 4.1: SOBOL analyses for the final, peak, and time of peak value, without a washin and washout rate. The input value ranges to test each parameter used for this SOBOL test can be found in Table E.3, except washin and washout is 0.

4.3 Initial Value Analysis Results

Figure 4.2a and Figure 4.2b illustrate how varying the initial uninfected bacteria population from 1 to 500 (using 100 different starting values) affects the dynamics and time of peak population of phage and total bacteria populations using the 95% rule.

Figure 4.2a perfectly replicates Figure 1 of Mulla et al. [43]. As the initial bacteria population increases, the time to reach the phage and bacteria sum peak decreases, following $y = -0.8648 \cdot \ln(x) + 9.7911$ and $y = -1.0056 \cdot \ln(x) + 7.7626$, with $R^2 = 0.9800, 0.9988$ respectively.

Figure 4.2b on the other hand shows different behavior. As the initial bacteria population decreases from 500 to 100, Figure 4.2a exhibits the same behavior. There is a change in behavior at 100 and less initial uninfected bacteria. Instead of following the predicted line like in Figure 4.2a, the curve for the phages suddenly decreases, following a non-monotonic curve. The bacteria on the other hand plateau before starting to increase again. The fitted curves follow $y = -0.1292 \cdot \ln(x) + 10.1462$ and $y = -0.6234 \cdot \ln(x) + 6.9602$, with $R^2 = 0.5406, 0.9206$ respectively. The slope tells us how well the uninfected bacteria has an influence on the time of peak value. The larger (positive or negative) the slope is, the more impact the uninfected bacteria had on the time of peak value. The closer the R^2 value is to 1, the more proportion of the variance for the time to peak value is explained by the uninfected bacteria. There is a deviation because the model changes limiting regions.

Images/Plots/Created/IVA/initial_value_analysis_UB_50_500_a_good_plot_2.png

(a) IVA for Table E.2. Replicates Figure 1 of Mulla et al. [43]. The system is adsorption limited [43].

Images/Plots/Created/IVA/initial_value_analysis_UB_50_500_a_good_plot.png

(b) IVA for Table E.1. For uninfected bacteria less than 100, the phage-bacteria interaction is resource limited.

Figure 4.2: Varying the initial uninfected bacteria concentration, from 50 to 500, with 30 unique values tested. Varying the default parameter values a can have a large influence on how changing the initial bacteria concentration influences the dynamics of the system. The default values for Figure a) and b) can be found at Table E.1 and Table E.2.

4.4 Phage Proliferation

4.4.1 Phase Portrait

Figure 4.3a shows a phase portrait varying the initial resource and phage concentration. The same initial phage values have the same color for the line. For phages that start above 25.98, the phage population can proliferate until the washout would eventually remove the phages. For phage populations that start below 25.98, the washout removes the phages before the phages had time to infect and kill the bacteria. Both regions of phages exhibit consistent behavior, of either going to 0 or proliferating. If the phage population started at exactly 25.98, if the initial resources was 260 or above, the phages died out. If the initial resource value was 255 or below, the phages proliferated.

4.4.2 An Initial Phage and Resource Analysis for Phage Proliferation

Figure 4.3b expands on the phase portrait by simulating more values and coloring the square depending on if the phages proliferated or not. The initial resource values span from 1 to 500, and the initial phage values range from 25.5 to 26.5, each with 100 unique values sampled. A boundary between the non-proliferating and proliferating phages can be curve-fit following $y = \frac{86.756x}{15.811+x} - 10.241$ with an R^2 value of 0.994.

Figure 4.3 zooms into the range (1–40, 24.2–25) for a high detailed view of the behavior happening around initial resources of 10. From 1 to around 7 initial resources, fewer phages are needed to proliferate. At 7 initial resources, there is a minimum in the phage proliferation boundary. From 7 initial resources and upwards, as more resources are added to the system, more phages are needed to ensure proliferation. Despite this, the change is tiny, a difference of about 2 phages. Considering the range of possible initial phage populations, the phage proliferation boundary is essentially flat. Under these parameter values, choosing an initial phage population of 27 or higher will ensure phage proliferation. This behavior is counter-intuitive. It would be expected that as there are more resources, the bacteria would have more resources to consume, allowing more phages to grow. A reason for this behavior might be because as there are more resources, bacteria can grow faster. The bacteria growth population outpaces the growth rate of the phages, causing the phages to die out due to the washout.

If there is a higher washout, similar behavior is observed where the phage proliferation boundary exhibits a similar shape to that of Figure 4.3b, except more phages are needed to proliferate. If K is increased to a larger value, the minimum in the proliferation boundary is shifted to the right.

4.4.3 An Initial Phage, Bacteria, and Resource Analysis for Phage Proliferation

The initial resource concentration had some, but very limited impact on if the initial phage concentration would affect if the phages proliferate. Within the context of the basic Golding model, the initial uninfected bacteria population is one of three parameters that a researcher can easily control, with the other two being the initial resource and initial phage. For low initial uninfected bacteria populations, it will be harder for the phages to proliferate. There is not enough bacteria to infect before the washout will remove the phages from the system. While for large initial uninfected bacteria populations it will be easier for the phages to proliferate such that the washout won't immediately wash the phages out. So I extend the initial resource and phage population analysis by



Figure 4.3: Varying initial resources and initial phages and the resulting proliferation and fitted proliferation curve. The box is colored red if the phages proliferated for that condition, and white if the phages died out. Phages proliferated if they reached 2 times their initial population at any point in time in the simulation. This simulation used the values from Table E.2, but with washout set to 0.02 instead of 0.

adding a third dimension to the analysis, the initial uninfected bacteria population. The aim of adding the uninfected bacteria is to see how the initial uninfected bacteria will 1) affect if the phage can proliferate, and 2) affect the max population that the phages can reach.

Figure 4.4 has three axes, the initial phage, resource, and bacteria population value. The initial uninfected bacteria did not have a significant impact on the 1) if the phages would proliferate, and 2) by how much the phages would proliferate. If spliced along the bacteria axis, there is little difference in the shape of the curve. It was expected that as the uninfected bacteria count would increase there would be significantly fewer phages

that would be needed to ensure phage proliferation. However, there is not a significant change in if the phages proliferated and by how much.

This suggests that under a washout situation, ensuring that there are enough phages is the most important factor to ensure that the phages are not washed out.

Images/Plots/Created/PP/3d_plot_resource_bacteria_phage.png

Figure 4.4: 3D plot of phage proliferation, dependent on initial resource, uninfected bacteria, and phage population. Color scaling from white to red, color is dependent on the max phage population reached.

4.5 Plotting Parameter Change — $3 \times 2 \times 3$ Model

Now that we have identified the most important parameters in the Golding model, we can analyze how the curve shapes change across a range of parameters for a larger model. The larger model will exhibit different behavior than a $1 \times 1 \times 1$ model due to the many interactions. The differing parameter values across each interaction will influence how fast each population can grow and die. A $3 \times 2 \times 3$ model was chosen as it is on the boundary between adding more phages, bacteria, or resources would clutter the plot with lines, while still offering behavior that can be compared against one another. The graph network that was used can be found at Figure 3.1b, with the default parameter values found at Table E.4. B_0 is infected by P_1 and P_2 , and consumes R_0 and R_1 . B_1 is infected by P_0 and P_2 , while consuming R_2 .

Figure F.3, Figure F.4, and Figure F.5, show a 7×7 matrix of subfigures across washout rates of 0, 0.02, and 0.05. Each subfigure uses a different combination of r and β parameter values. However, we will specifically focus on Figure 4.5a, Figure 4.5b, and Figure 4.5c. All initial phage values started at 10. This was specifically chosen to show how even though the phage values all start the same, the different parameter values and interactions ultimately influence the population growth.

If r or β is equal to *Original*, then the simulation uses the original parameter values as defined in Table E.4, otherwise each r and each β parameter interaction has the value listed in the subfigure title.

The columns and rows of each figure show how a change in parameter value affects the curve, while keeping the other parameter the same. In $r, \beta, \omega^o = \text{Original}, \text{Original}, 0$, although not a realistic growth curve, shows how the different parameter values for each interaction uniquely affect the growth rate of each entity, especially the phage population (P0=blue, P1=green, and P2=purple). Despite all phages starting at the same population level, within the first two or so time units, P1 has less phages than P0 and P2. P2 has the fastest initial growth rate, as P2 has the most phages until $t = 4$, at which point P1 has a larger phage population. P2 reaches its peak population count before P0 or P1, but despite the slower initial growth, P0 and P1 eventually overtake P2 in total phage population. P2 also actually reaches its peak before decreasing in population. Since the phage population is reduced by $r_{pb} \cdot (U_b + \sum_{k=1}^M I_{b_k})$, and by specifically choosing the parameter values as used in Table E.4, behavior that hasn't been seen in a $1 \times 1 \times 1$ system has been found. The complete extinction of the bacteria has been delayed long enough such that at trace amounts, there is phage reduction despite bacteria still existing. The peak times for P0, P1, and P2 are $t = 6.33, 7.99, 4.52$, a difference of 3.47 time units.

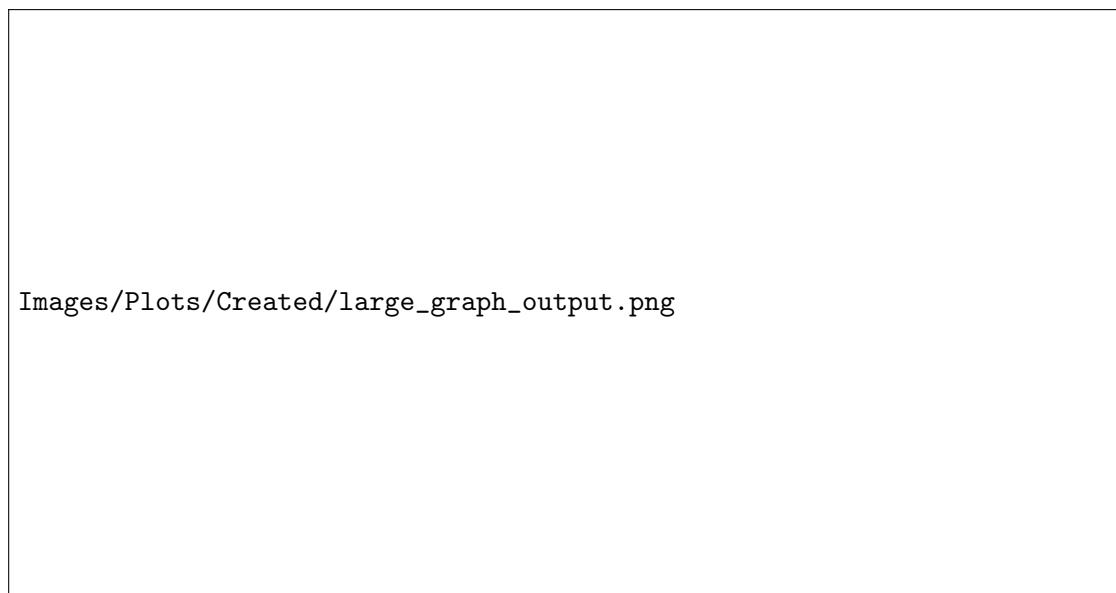
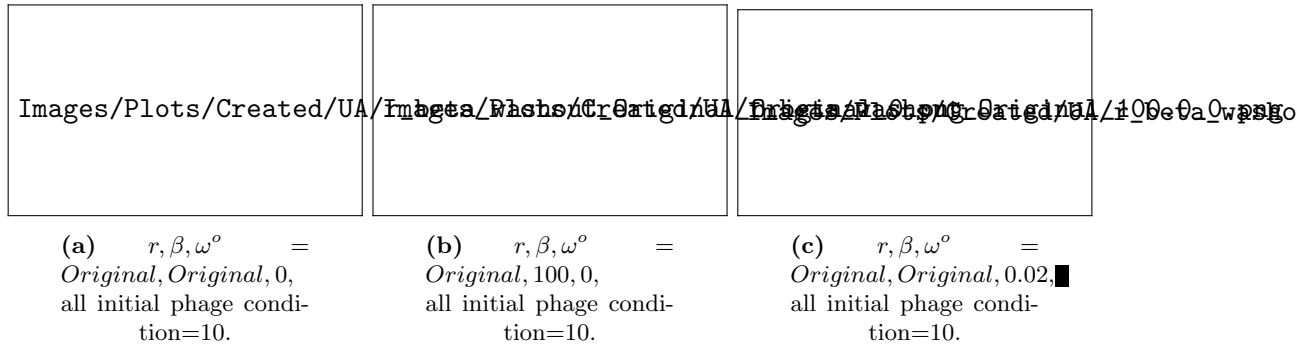
Contrast that with the phage population dynamics of that with $r, \beta, \omega^o = \text{Original}, 100, 0$, the phage populations do not show interesting dynamics. The peak times are more similar and consistent to one another ($t = 5.50, 7.01, 6.78$, a difference of 1.51 time units). The phage population curve all appear the same, with slightly slower growth rates. There is no crossing of phage populations unlike with $r, \beta, \omega^o = \text{Original}, \text{Original}, 0$.

The highlighted example demonstrated the dynamics and influence that multiple agents can have on the final output.

The top row of Figure F.4 shows how the phages and resources died out relative to the top row of Figure F.3. Even with a high burst value, the phages could not defeat the pressure from the washout. But by changing the r value from $r = 0.001$ to $r = 0.041$, the phages were able to save themselves and proliferate.

4.6 Phage and Bacteria, Survivability Analysis For A $20 \times 20 \times 10$ System

Using the simulation framework, I created and analyzed a $20 \times 20 \times 10$ system. I selected two parameters, τ and β , to run a survivability analysis using the extended Golding



model. Each phage is guaranteed to interact with at least one bacterium but no more than two bacteria. Each bacterium interacts with at least one phage and one resource, but not more than two phages and two resources. Every resource interacts with at least one bacterium, and at most three bacteria. The parameter values were randomly selected from a uniform distribution in the SOBOL analysis value ranges (Table E.3). A phage survived if its final population is greater than 1 at the end of the simulation.

Chapter 5

Discussion

This section presents an analysis and discussion of the results.

5.1 Graph Behavior

Table 4.1 presents illustrative examples rather than a comprehensive analysis. The behaviors shown represent typical trends observed when varying each parameter in the specified direction, but they may not apply to all possible values or reflect the magnitude of changes. Additionally, these results do not necessarily generalize to scenarios where two parameters are simultaneously varied. Table 4.1 should be interpreted alongside the local $S1$ sensitivities from Section 4.1 to better understand how sensitive the output is to specific parameters and the potential impact of their variation.

Many parameter changes offered little substantial changes in graph behavior. The changes were mostly minor with not a significant change noticed. A change in parameter input would sometimes result in 50-100 fewer phages compared to the original reference graph. The magnitude of change is roughly in line with the SOBOL results.

As an example take τ from Table 4.1 and Figure 4.1. I noted that for $\tau = 3$ the phage and total bacteria peak was significantly later than for the default τ value of 2.14. Likewise for $\tau = 0.5$, the phage and total bacteria peak occurred significantly earlier than the reference graph. Looking at τ in the Phage and Total Bacteria Peak Time figure, Figure 4.1c, τ has a significant impact on the peak time.

A biologist would look at the growth curve and create their conclusions by visually looking at the curves and reasoning through the ODE model to explain the behavior. A biologist can supplement this analysis with a SOBOL analysis to quantify how significant the change was, and compare a parameter's significance with other parameters.

5.2 A Realistic Growth Curve

As the bacterial population grows, resource consumption accelerates until only trace amounts remain. The delay between the peaks of uninfected and infected bacteria is due to the infection stages and the latent period of phage infection. Each bacterium transitions from infection stage k to $k + 1$ at a rate of $\frac{M}{\tau}$. Therefore, decreasing the number of infection steps M or increasing the latent period τ amplifies this delay. A longer latent period means it takes more time for bacteria to progress through the infection stages.

At $t = 4$, the infection rate surpasses the bacterial replication rate, causing the bacterial population to decline even though resources are still available. This moment coincides with the rise of the phage population. Observing the timing of these events and changes in the graph's behavior, as well as their relationships across different graphs, helps clarify the complex population dynamics and the interdependence of the populations. The nature of the models being nonlinear makes the analysis harder to understand and conceptualize.

Understanding the system becomes more complicated as the model increases from a $1 \times 1 \times 1$ system to a $p \times b \times r$ system. Now up to any number of phages can interact with any number of bacteria, and any number of bacteria can interact with any number of resources, each with their own unique parameter values. These varying rates will significantly influence the dynamics of the system, and make it hard to determine what event caused what due to the rise in number of interactions. There are only 2 interactions that occur in a $1 \times 1 \times 1$ system. With a $p \times b \times r$ system, there are at most $p \cdot b + b \cdot r$ interactions that can occur. So many individual events occurring at the same time makes it harder to identify the cause of the event, and how the event's action will propagate through the network. A method to circumvent this issue is by knocking out certain nodes or edges and rerunning the simulation and compare the results. The knocked out node or edge won't contribute to the simulation anymore, so there will be an impact on the population count.

5.3 SOBOL Sensitivity

SOBOL, when mixed with a qualitative analysis can provide insight into why when a parameter changes, the output changes as it does. A researcher might look at an ODE model and reason through the changes. They might explore the model by having an internal monologue as follows. "If I increase τ , which means that the bacteria infection process takes longer, then when a phage infects a bacterium, it will take longer for the

bacteria to die. Dying later means that the phages are released later. By releasing later, it will take longer for the phages to grow and peak. It also allows more time for the uninfected bacteria population to grow and use up the resources. There will be a natural delay in uninfected bacteria peak as it takes longer for the bacteria to become infected and go through the infection process.”

A researcher might use SOBOL to quantify these changes, and use the analysis to gain a better oversight of the model. By identifying the important parameters, a researcher could engineer new phages to target those changes to alter the output in their favor.

5.3.1 Resources

Every parameter affects how the bacteria and phage population grows in some way, which influences the consumption rate of resources, which determines the final resource value. Of the other parameters, τ has the biggest influence because τ determines how fast the bacteria will go through the infection process. The longer it takes, the longer it takes for the phage population to grow, allowing more bacteria to grow and consume resources.

5.3.2 Phages

The r value quantifies how fast the phages infect the uninfected bacteria. r , the adsorption rate of phages to bacteria, can be interpreted as the efficiency of infection. The smaller the value, the more efficient the infection process is, and fewer phages it requires to infect a bacterium. With a larger r value, more phages are used to infect a bacterium. β has an influence on the final phage population, as the infected bacterium will release β phages into the system. The more phages that are created for every lysed bacterium, the more phages are available in the system.

The barplot values for the peak value for phages using the 95% rule has the same values as in the final value plot for the phages. This makes sense as there is no removal of phages from the system, so any phages created by r or β will stay in the system. As the population is ever-increasing, the final and peak value will be occurring near one another and are tightly associated with one another.

The τ parameter influences how fast an infected bacterium goes through the infection process. Decreasing tau increases the speed of lysis, allowing more phages to be produced faster. This in turn will increase the phage population faster than other parameters, meaning that the phages reached the peak population faster. r and β have similar effects, but rather have a larger effect on the final and peak phage population than the

time it takes to reach the peak value. r and β add to the phage population, rather than specifically speed up a process which τ does. Decreasing r and increasing β lead to more phages being created, which can then infect more bacteria. This won't have nearly as large of an impact as shortening the infection period, literally decreasing the time until new phages are created, thus causing the phage population to reach its peak faster.

5.3.3 Total Bacteria

Resources, τ , e , and β all play a critical role in the final population value of bacteria. More resources allow bacteria to grow for a longer time, allowing more bacteria to be created. β has a very important role in determining the final bacteria population, but surprisingly r has no role in determining the final bacteria population. e determines the resource consumption rate. The larger e is, the faster the depletion rate of the resource. So by lowering e , more bacteria will be created, and the time at which the bacteria peak at occurs later in time. Of course as β changes value, it will have a large influence on the final bacteria population. More phages will cause more infections, slowing the spread of bacteria. However, r surprisingly does not have an influence on the final bacteria population level.

The total bacteria peak population is much more sensitive to the different parameter values. The bacteria act as a link between the phages and resources. Any changes in the resource consumption rate or initial condition will affect the bacteria population. Likewise, any change in phage adsorption rate will affect the bacteria growth, which in turn will affect the resource consumption rate. The bacteria have the ability to dampen the effect of certain parameters. For example, the initial resource value affects the final resource value. The initial resource value partially affects the final bacteria value, but it doesn't affect the phages. The parameters lose strength as it propagates through the system.

Since the bacteria exist in the middle between the phages and resources, the bacteria are exposed to many different parameters that will ultimately influence the peak value. Many of these parameters are interacting with one another hence why $ST > S1$ is true for many of the inputs.

Similar to the peak value, the bacteria interact with many parameters, who interact with other parameters. The time of the peak can only occur between $t = 0$ and the end of the simulation, limiting the values that can be measured, reducing the potential variance seen in the output. The peak value on the other hand has no limit on the peak value, with a peak value occurring anywhere between 0 and ∞ . e and K depend

almost exclusively on higher order terms due to the nature of the bacteria growing at the Monod rate.

5.4 Initial Value Analysis

The behavior between Figure 4.2a and Figure 4.2b should be similar, however the change in parameter values altered the simulation to introduce a region in behavior change. It would be expected that for 100 initial uninfected bacteria and less the bacteria sum peak time would follow the linear regression line, but at around 100 uninfected bacteria and less, the peak curve deviated from the linear expression.

Between 100 and 500 uninfected bacteria, the system is adsorption limited. The adsorption of phages to bacteria depends on the bacterial concentration [43]. There are not enough phages relative to the population to infect the bacteria, so the phages slowly adsorb to the bacteria. The bacteria can grow without immediate pressure from the phages. There is also a lack of resources which is restricting the bacterial growth. For large initial bacteria concentrations, the resources run out. This severely limits the ability for the bacteria to grow and artificially limits the population cap of the bacteria.

The system is latency limited between 25 and 100 uninfected bacteria. The collapse time in a latency limited regime is independent of the initial bacteria population [43]. As the initial bacteria decreases, the phage to bacteria ratio increases, and they can infect the bacteria faster. So the time to phage peak also decreases as the initial uninfected bacteria decreases.

As the uninfected bacteria decreases from 25 towards 1, it takes longer for the bacteria to grow and reach their peak population count. At these initial bacteria concentration levels, there is enough resources to fully sustain the bacteria through the whole simulation. For uninfected bacteria less than 25, the system enters a new sort of restriction, where the system experiences a delayed infection due to low encounter rates.

The transition rate from U to I_1 is proportional to $U \cdot P$. Fewer bacteria are initially infected with a low initial starting bacteria. If the phages can't infect the bacteria, the later infection stages are delayed due to the slow infection process. There could be a threshold for phage to uninfected bacteria where a certain dilution rate will significantly affect the peak time. This value could be around $\frac{\text{initial phage}}{\text{initial bacteria}} = \frac{10}{25} = 0.4$ as at around 25 uninfected bacteria is when the system switches from latency limited to the new limited regime. The bacteria have a longer amount of time to grow as there is a low infection rate and plenty of resources to consume. This means that it takes longer for the bacteria to grow, as noticed by the increase in peak time relative to larger initial

uninfected bacteria populations. As the bacteria population drives the phage population, an increase in bacteria time of peak causes an increase in phage time of peak.

5.5 Phage Proliferation

5.5.1 Phase Portrait

There is non-linear trade-off between initial resources and initial phages when there is washout included. The washout non-linearly affects if the phages proliferate or not. The bigger the washout value, the harder it is for the phages and bacteria to proliferate. The bacteria couple the phage populations to resources, so changes in initial resource concentration will have an effect on the final phage value. Increasing the initial resource concentration creates more bacteria, while decreasing it results in fewer bacteria. More bacteria ultimately produce more phages, while fewer bacteria ultimately result in fewer phages. While SOBOL with washin and washout, Figure F.1b, showed that the final value for phages due to changes in initial resource input values is limited (sensitivity ≈ 0.1), it still has an impact.

For low initial resource concentration values, values below 10 the resource, the Monod curve is below the half-velocity constant (the velocity v is 1 and K is 10). The lack of resources restricts the bacteria growth, and the bacteria can't grow quickly. As the resource concentration increases towards $K = 10$, the bacteria can grow faster. Since K is small, a small change in R causes a relatively large change in the Monod rate.

At around the minimum in the phage proliferation boundary, the behavior changes. At $R \approx 7$, the Monod rate reaches half of its max velocity. This behavior should be seen at around 10, but the washout has an effect on the Monod rate by artificially shifting the point where the half velocity occurs from $K = 10$ to $K \approx 7$. $10 \cdot 0.98^{15} = 7.386$

As R increases from K , the bacteria are not limited by the nutrients anymore and can grow faster. However, as R increases beyond K , each additional unit of R results in a diminishing increase in the Monod rate, which asymptotically approaches its maximum velocity. As bacteria grow according to the Monod equation $g(N, v, K)$, the phage population dynamics remain tightly coupled to bacterial growth.

Phage proliferation becomes a race against time under external pressure. The phages will not proliferate if the phage growth rate is not fast enough to initially beat the washout removal rate, or the infected bacteria are washed out before lysing.

5.5.2 3D Plot

It is difficult to see inside the matrix, but using the color on the outside can give some insights into the behavior happening inside the matrix. Even with the added bacteria, the phage proliferation boundary is still heavily dependent on the initial phages and initial resources, and less so on bacteria.

5.6 Plotting Parameter Change

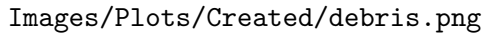
5.7 Large $20 \times 20 \times 10$ System

There are so many interactions and parameters in large and complex systems that it becomes hard to analyze. There is no clear overview of the model, and a figure of the network interactions and a copy of the parameter inputs is needed in order to have some sort of chance to analyze why an entity is behaving as it does. It is hard to simplify the model as each entity is influenced by the sum of other entities that it interacts with. The lines for each population curve cover the other lines, and some lines have the same color due to limited color ranges.

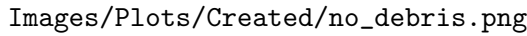
A recently published paper Dey et al. [60] uses the Golding model but adds a new term, debris. While running their simulations and experiments, the model's results would diverge from their experimental work. Their thinking is that freshly lysed bacteria still have biomarkers that phages can detect and attach to. Incorporating the debris term, which acts as an additional sink for phages, improved the model's alignment with the experimental data. The phages think they are infecting a bacterium, but in reality they aren't. The debris term can also encompass bacterial phage defenses (Section 2.3). The phage equation from the Golding model can be rewritten as

$$\frac{dP_p}{dt} = \sum_{b \in B} \beta_{pb} \cdot \frac{M}{\tau_b} \cdot I_{b_M} - r_{pb} \cdot (U_b + \sum_{k=1}^M I_{b_k}) \cdot P_p - w^o \cdot P_p - d_{p,b} \cdot P_p$$

Figure 5.1a shows how the effect of the debris term d has on the growth curves of the phages and bacteria in comparison to no debris term, Figure 5.1b. Without the debris term, only one uninfected bacteria survived, and every phage survived except for one phage who died due to the washout. Three uninfected bacteria species reached more than 1000 uninfected bacteria at any point in the simulation time, and only two infected bacteria species reached more than 1000 infected. The maximum total bacteria population that was reached was a total of 6620 bacteria.



(a) The $20 \times 20 \times 10$ model with a debris factor included.



(b) The $20 \times 20 \times 10$ model without the debris factor included.

Figure 5.1: A large $20 \times 20 \times 10$ model with a debris model added. The debris parameter values were randomly and uniformly selected between 0.01 and 0.2.

With the debris term included, the behavior is slightly altered. Three uninfected bacteria survived, four different uninfected bacteria strains ever reached a population value of greater than 1000 at any point in time during the simulation. Only one bacteria strain ever reached more than 1000 infected bacteria, The ending bacteria value is 12000, almost double the maximum bacteria population reached without debris. On average, there were significantly fewer phages at the end of the simulation than without debris. No phage population ended above 2000 with debris, while without debris two phage populations ended up with more than 2000 phages.

It is clear to see that debris has a significant impact on the dynamics of the system. There are in general fewer phages to infect the bacteria with the additional removal of the phages. Fewer infections mean more uninfected bacteria and fewer phages being produced. This feedback loop keeps on going until the end of the simulation where it is possible to see the differences in behavior.

Chapter 6

Conclusion and Future Work

6.1 Conclusion

Understanding the relationship that phages have with bacteria and the environment is complex. Even for a $1 \times 1 \times 1$ system, the system is already complex. Not including M and the initial infected bacteria population, the parameter input space is 12 dimensions large. Although quite small in comparison to other larger models, analyzing 12 unique parameters and their interactions takes effort. Finding parameter values that result in quality graphs is not the easiest task, although knowing the expected values and the biological relevance makes the task easier. Finding a set of parameters that results in behavior that is worth analyzing takes time. Using interactive graphs like what I created helps the user to look through the parameter space to find interesting behavior and gain a deeper understanding of the model. However even a simple change in the parameter input like in Figure 4.2b vs Figure 4.2a shows vastly contrasting behavior, despite both graphs being realistic.

Trying to expand an analysis into a $p \times b \times r$ system becomes even more complicated due to the interconnected nature of the entities. With larger and larger systems small changes in a single parameter will not have big of an influence on the final output. But if the parameter value does have an influence, it has a cascading effect on the whole network. Increasing the infection rate of phage 1 will slow the growth of the bacteria 1. With slower bacteria 1 growth, phage 2 is affected as there are less bacteria 1 to infect (assuming that phage 2 can infect bacteria 1). With lower phage 2 count, bacteria 2 can grow, using more resources. The

And how do you change the parameter value of the vector or matrix representation? If you want to change τ to 1.5, how do you do that? Do you only change one value in the

vector or matrix, so for example $\tau = \begin{bmatrix} 1.43 & 0.98 & 1.13 \end{bmatrix}$ becomes $\tau = \begin{bmatrix} 1.5 & 0.98 & 1.13 \end{bmatrix}$? Do you set each value in the vector or matrix the same, so $\tau = \begin{bmatrix} 1.43 & 0.98 & 1.13 \end{bmatrix}$ becomes $\tau = \begin{bmatrix} 1.5 & 1.5 & 1.5 \end{bmatrix}$? Do you respect the different values in the vector or matrix by shifting the values from the average value? So $\tau = \begin{bmatrix} 1.43 & 0.98 & 1.13 \end{bmatrix}$ becomes $\tau = 1.5 - \frac{1.43+0.98+1.13}{3} = 1.5 - 1.18 = 0.32 = \begin{bmatrix} 1.43 + 0.32 & 0.98 + 0.32 & 1.13 + 0.32 \end{bmatrix} = \begin{bmatrix} 1.75 & 1.3 & 1.45 \end{bmatrix}$. How does that change if the value is 0? Do you skip it and don't let that value count towards the average value to shift the vector and matrix values by.

6.2 Future Work

Next steps would be to give the model to the lab technicians running lab experiments so that they can verify the results as seen in the output by comparing the lab results with the model output. With the lab results, the model can be adapted to better fit the lab results. This can be done by changing parameter values, or by changing the model equation. The user can decide to add the Monod microbial growth model to the growth of the bacteria, or adapt the Monod equation to being dependent on multiple sources. Using the model, the technicians can improve and validate their methods. If the empirical results significantly deviate from the model results, the technician can review to see if their method is appropriate and follows protocol. They might have accidentally not added enough resources, or accidentally miscalculated the initial concentration of bacteria.

6.2.1 Other Models

There are numerous considerations to account for when modelling phages and bacteria, with numerous ways to go about the considerations. Each model has its pros and cons. Take the exponential population growth model

$$\frac{dP}{dt} = rP \quad (6.1)$$

$$P(t) = P_0 e^{rt} \quad (6.2)$$

where $P(t)$ is the population at time t , P_0 is the initial population, and r is the growth rate. This model acts as a nice introduction to population modelling. It can accurately fit the exponential growth bacteria experience in a petri dish. However, this basic model does not account for a spatial and resource consumption. Eventually the bacteria run out of space and resources, and start to die out. A population can not grow exponentially forever, the resources can only support a maximum population, the carrying capacity.

Images/Plots/Created/exponential_vs_logistic_growth.png

Figure 6.1: Exponential growth curve vs logistic growth

The model can be adapted to include a carrying capacity (the max population level that can be reached), where the new updated model is

$$\frac{dP}{dt} = rP\left(1 - \frac{P}{K}\right) \quad (6.3)$$

$$P = \frac{K}{1 + \left(\frac{K-N_0}{N_0}\right)e^{-rt}} \quad (6.4)$$

where K is the carrying capacity. This adapted model, the logistic growth model better accounts for the eventual restriction of population growth.

Figure 6.1 shows how the carrying capacity has a large influence on the speed and growth trajectory of a population. The logistic curve initially follows the exponential curve before the maximum growth rate is reached and starts to slow down and taper off as the population asymptotically approaches the carrying capacity $K = 200$.

A further step would be to introduce competition between other bacteria. For example, a $p_{0,1} \cdot P_0 \cdot P_1$ term can be subtracted from the logistic growth curve. This term accounts for competition between Populace 0 and Populace 1, with $p_{0,1}$ being the interaction factor between P_0 and P_1 . Assuming P_0 is being looked at and P_0 has a high value, if P_1 is high, then a lot of P_0 is going to die out due to the competition with P_1 . If P_1 has a low population, then not many P_0 are going to die out due to less competition with P_1 .

The model can be further extended by accounting for temperature, pH, more interactions between other entities, the constant addition and removal of other entities, and other considerations.

6.2.1.1 Model Replication

Peer review is very important in research. So being able to replicate other models like that of Nilsson [4] is another way to further extend this research. A benefit of

implementing Cocktail's model is that it would be possible to model multiple bacteria and phages at the same time, as noted as a limitation in Section 2.7.3. The model can also be adapted by introducing new environmental factors like pH or UV. Cocktail supports adding more phages at set times, but only at most three times. The model can be extended by allowing more times when phages can be added.

6.2.1.2 Debris

Looking further into the debris and its effects would be a next step in the project. It was casually shown how adding a debris term increased the survivability of the bacteria populations, with showing on average a higher uninfected bacteria population, and lower uninfected and phage population count.

6.2.1.3 Spatial simulations

<https://www.sciencedirect.com/science/article/abs/pii/S0022519318305368> The ODE models work very nicely when there is no consideration for space and 2D/3D-space dimensionality. Spatial models complicate the simulation, making it harder to analyze. Data collection and analysis becomes harder. Unique and novel analysis and visualization methods have to be created to be able to represent and visualize the data through space and time.

PDE PDE can be used to add space to an ODE model. The general formula, as given by

$$\frac{\partial u}{\partial t} = D\nabla^2 u + f(u, x, y, \dots, t)$$

where $u(x, y, \dots, t)$ is the population density of interest, D is the diffusion constant, ∇^2 is the derivative of each spatial direction, and $f(x, y, \dots, t)$ is the function encapsulating growth, death, and interactions dynamics. Modelling the localization of phages on a petri dish would be of interest.

Discretization The dimensions can be discretized into boxes of dimensions $\delta x, \delta y, \dots$. This transforms the PDE into a system of difference equations, which can be solved numerically. For example, the Laplacian term $\nabla^2 u$ in 2D can be approximated using finite differences as:

$$\nabla^2 u \approx \frac{u_{i+1,j} - 2u_{i,j} + u_{i-1,j}}{\delta x^2} + \frac{u_{i,j+1} - 2u_{i,j} + u_{i,j-1}}{\delta y^2}$$

where $u_{i,j}$ represents the value of u at the grid point (i, j) . This discretization allows the PDE to be solved iteratively over a grid, enabling spatial simulations of population dynamics. Each box can be represented by a matrix, and the population value can be displayed as a heatmap using visualization software.

6.2.2 Lab Work

A next logical step would be to complete lab work to obtain curves that could be used to compare the simulation results with the lab results. If the curves are significantly different from that of the ODE model, a new ODE model can be created. Curve fitting algorithms can be used to numerically find the interaction parameters for the new ODE model. Using the simulation software would save time, money, and resources as fewer experiments would have to be run.

The lab work would act as an important model validation step. Dey et al. [60] showed how their ODE model would eventually diverge from the lab-produced ODE curve. They were able to achieve a better curve fit by adapting the model to include the debris term.

Future lab work can also include finding out which bacteria, phages, and resources are found in marine water via samples taken from the environment. The next step would be to build an interaction network, along with experimentally finding out the interaction parameter values using experimental lab work. Researchers can predict how the system would behave under new untested conditions, saving money and time. It might also tell researchers if they made a mistake during testing. If the model says the system should behave in one way, but the system acts differently, the researcher can review their methods and maybe make changes to how they run the experiments. All in all, having a model that takes seconds to run will help aid researchers better understand the system.

6.2.2.1 Environmental Modelling

Many results in research papers come from controlled lab settings. As a next step, researchers can actively collect daily water samples and measure phage, bacteria, and resource concentrations. Collecting samples for over a year would create an ODE-like population curve of the entities. This approach would provide deeper insights into the dynamics of bacteria and phage populations in natural environments, at the loss of control over conditions. By continuously monitoring environmental factors such as hourly temperature, rainfall, and the concentrations of each entity, researchers can gain a deeper understanding of the causal relationships within the ecosystem. By conducting

the experiment over the course of a year, short-term fluctuations in daily measurements are averaged out, resulting in a smoother overall curve.

Chapter 7

Ethics and Data Management

7.1 Ethical Considerations

There are some ethical considerations needed. Phages can be used to treat bacterial infections, and may need to be safely administered under the supervision of a doctor, despite little to no side effects on the patient. Trying to control phages either in food or in the environment by releasing a phage cocktail into waterways could potentially cause issues further down the line if the released solution contains unwanted chemicals. An extra step in the food production will increase food costs and make food production harder to control. The cost to create, maintain, and use phages at an industrial size can become costly and require a lot of energy. Dumping phages into the ecosystem could potentially cause issues if the phage concoction includes resources for the bacteria to use, and can become costly for taxpayers.

7.2 Data Management

All data and results can be found on GitHub. Some simulation data will have to be recreated as the *.parquet* datafiles are too big for GitHub to store. Measures have been taken to label and document the code, datasets, parameter configurations, and for example with Appendix E. Any qualified researcher should be able to replicate, audit, use, and edit the computational experiments and code if needed. This systematic approach to version control and storage aligns with best practices, ensuring that results are both traceable and verifiable.

7.3 Adherence to Codes and Principles

I acknowledge that the thesis adheres to the ethical code and research data management policies of UvA and IvI.

The following table lists the data used in this thesis, with the source code. I confirm that the list is complete and the listed data are sufficient to reproduce the results of the thesis.

Short description (max. 10 words)	Availability (e.g., URL, DOI)	License
Dataset	Simulation Results	MIT
Source Code	Source Code	MIT
Simulation Conditions	Appendix E and text under figures	

Appendix A

Appendix A: Equation Parameters

Parameters used in the various equations.

A.1 Simple/Advanced Golding Model Parameters

A.2 SOBOL Parameters

A.3 Linear Regression Parameters

Variable	Name	Description
P/P_p	Phages entity	Phage population for phage p
U/U_b	Uninfected Bacteria entity	Uninfected population for bacteria b
I_i/I_{b_i}	Infected Bacteria entity	Infected population for bacteria b at stage $1, \dots, i, \dots, M$
B/B_b	Bacteria entity	Total bacteria population for bacteria b , assuming $B_b = U_b + \sum_{i=1}^M I_{b_i}$
R/R_r	Resource entity	Resource r concentration
e/e_{br}	Consumption rate	Rate at which resource r is consumed by bacteria b
β/β_{pb}	Burst size (B matrix)	Lytic burst size for phage p and bacteria b
r/r_{pb}	Successful phage/cell encounter	Probability of a phage p successfully infecting bacteria b
τ/τ_b	Latent period (tau vector)	Time it takes bacteria b to go through one infection stage
v/v_{br}	Maximal growth rate	Growth rate of bacteria b from resource r
K/K_{br}	Monod Constant	Monod constant representing the resource r concentration at which bacteria b grows at half its maximal rate
ω^i/ω_r^i	wash-in rate	Rate of resources r being added
ω^o/ω^o	wash-out rate	Rate of entities being removed, acts on all entities equally
M	Number of infection stages	Number of infection stages that a bacteria goes through, all bacteria entities have the same value for M
t	time	time value

Table A.1: Golding model parameters with variables, names, and descriptions. Subscripts on parameters indicate relationships; for example, e_{br} is nonzero if there is an edge connecting bacteria b to resource r in the network, zero otherwise.

Variable	Name	Description
Y	Univariate parameter output	univariate model output, such as mean μ or variance σ
X	Input vector	Vector of size d , input vector to f
i	Parameter input	Parameter i of input
X_i	Parameter value	Value of vector X at position $i = 1, \dots, d$, the value of parameter i
d	Input size	Size of input vector X
$X_{\sim i}$	Parameter input	All values of X that are not X_i
f	Function f	Arbitrary black-box function describing model
N	Samples	Number of samples, power of 2, 2^x
D	Parameter input size	Number of parameters inputted into SOBOL, $d = X $
ST_i	Global sensitivity	Contribution of parameter X_i to output variance of Y due to interactions with other variables
$S1_i$	First order sensitivity	Contribution of X_i to output variance of Y

Table A.2: SOBOL parameter symbols, name, and description.

Variable	Name	Description
a	Slope	Slope of the linear regression line
c	Intercept	y-intercept of linear regression line
R^2	Regression Coefficient	Coefficient of determination of linear regression fit, quality of regression
x_i	Data point	Data point on the x-axis
y_i	Actual Value	Actual value of data for a given x_i
\hat{y}_i	Predicted Value	Value predicted of equation for a given x_i
\bar{y}	Average Value	Average y value
n	Number of samples	Number of samples being tested

Table A.3: Variable symbol, name, and description used for the linear regression.

Appendix B

Appendix B: Industrial and Real Life Applications of Phages

Due to the nature of killing bacteria, there are numerous applications where a researcher or an organization might be interested in controlling bacterial populations.

A Food Safety Specialist might be interested in introducing a solution containing a high concentration of phages during food production to prevent the spread and growth of *Salmonella* or *E. coli* in the pet food. Alternatively, the Food Safety Specialist might want to promote beneficial bacteria like *Streptococcus thermophilus* used in the production of Emmental cheese, which heat would kill when the milk undergoes the pasteurization process.

A doctor might be interested in providing swallowable pills, more commonly known as phage cocktails, to a patient with a bacterial infection. There is evidence that phage-resistant bacteria are more susceptible to antibiotics, so the doctor might prescribe both medicines to effectively deal with the infection.

An Environmental Protection Officer might be interested to see how they can use phages to stop the spread of *Cyanobacteria* blooms in waterways, more commonly known as blue-green algae, a photosynthetic microscopic organism that is technically a type of bacteria. This would keep waterways safe for boating and swimming activity, aquatic life, and water consumption in farms, factories, and homes.

When there are a few known bacterial strains, a targeted concoction of phages can be used to control the bacterial population growth in any setting, either be it food, healthcare, or environmental. Phages offer properties of microbial control that other methods do not, making them an ideal candidate for some applications.

B.1 Controlling Foodborne Bacteria

Foodborne diseases are one of the primary ways for bacteria to spread to humans and animals. Some bacteria use the food as a vector to infect hosts, while some bacteria will deposit toxins on the food that is then ingested. If consumed in large enough quantities, or further produced in the host, the toxins can be fatal to the host.

Methods exist to control bacterial growth, for example by storing food below 5°C or above 60°C. Bacteria need moisture to grow, so starches like rice will have minimal bacterial growth. Bacteria prefer to live in slightly acidic to neutral pH environments, so having an environment that is extremely acidic like vinegar will prevent bacterial growth. The use of chemical antibacterial entities such as bleach is not desirable due to leaving chemicals on the food, which can be fatal if ingested. Physical entities like heat or radiation can kill bacteria, but at the cost of altering the food quality [61].

For example, *Streptococcus thermophilus* is one of three different bacteria strains used to create Emmental cheese. However, Emmental cheese does not use pasteurized milk, increasing the risk of *E. coli*. Emmental cheese producers can add phages that target *E. coli* to the milk during the production stage, while not affecting the bacteria used to produce the cheese.

B.1.1 Current Applications

Phage cocktails like SalmoFresh™ have been proven to safely reduce *Salmonella* contamination in pet food and raw pet food ingredients [6], as well as in romaine lettuce and bean sprouts [7]. Pet food contains meat and vegetables, where vegetables grown in or on the ground are at risk of *Salmonella* due to contact with soil, manure, compost, and other agricultural runoff from neighboring farms [18]. Figure B.1 and Figure B.2 show how application of phages have reduced the count of *Salmonella* in ingredients used in pet food as well as romaine lettuce and bean sprouts. In Figure B.1, each food group noticed at least a 68% reduction in CFU/g compared to the control when the 9×10^6 phage treatment was applied. There was at least an 80% reduction in CFU/g across all food groups when treated with a 9×10^6 or stronger phage solution. In Figure B.2, the lettuce and bean sprouts noticed a reduction of at least 0.6 log CFU/mL in *Salmonella* count across all temperature ranges. The smallest reduction in bacteria count in lettuce was noticed at 1 hour at 2°C with an absolute reduction in 62.0% between the control and treatment, while the largest reduction in bacteria of 90.0% was found at 72 hours at 2°C. For the bean sprouts, the lowest reduction in phages was found at 1 hour at 2°C with a reduction of 78.1%, and the largest reduction was 90.0% at 25°C after 48

hours. Although these values are still high above food safe, the ability to reduce the *Salmonella* population by at least 62% and up to 90% at different temperatures and incubation periods is impressive and can prolong shelf life, especially for foods that do not have long shelf lives before spoiling due to bacteria. As such, phages can be shown to control the spread of *Salmonella* in food sources and extend the potential shelf life of certain foods.

Images/Plots/Sourced/SalmoFresh_in_pet_food.png

Figure B.1: SalmoLyse[®] reduces *Salmonella* contamination on various food surfaces: Mean and standard error bars shown. Statistical analyses were carried out for each food group independently. Asterisks denote significant reduction from corresponding controls based on one-way ANOVA with Tukey's post-hoc tests for multiple corrections: ** denotes $p < 0.01$, while *** denotes $p < 0.001$ compared to the corresponding controls. There was significant reduction in *Salmonella* on all food surfaces with the addition of SalmoLyse[®] compared to the controls; the mean percent reductions from the control are noted in the boxes above treatment bars. CFU/g D colony forming units per gram. Each letter denotes a food group that was tested with SalmoLyse[®] and compared to a control: A= chicken; B= lettuce; C= tuna; D= cantaloupe; E= ground turkey. Plot sourced from Soffer et al. [6].

Images/Plots/Sourced/SalmoFresh_effectiveness_lettuce_sprouts.png

Figure B.2: *Salmonella* count in a mixture of 5 *Salmonella* strains spot-inoculated (CFU/g) onto a) lettuce and b) sprouts after spraying with a mixture of bacteriophage (SalmoFreshTM) relative to positive controls at 2, 10 and 25C and stored for 1, 24, 48 and 72 h. Plot sourced from Zhang et al. [7]

B.2 Phage Therapy and Antibiotics

Antibiotics are a common way to treat bacterial infections. However, antibiotics are not selective in the bacteria they kill, killing both harmful and beneficial bacteria. This can lead to the development of antibiotic-resistant bacteria, which makes it harder to combat that bacteria in the future. It has also been shown that antibiotics have a negative effect on the gut microbiome and brain development in mice. Phages are an alternative to antibiotics, as they are selective in the bacteria they kill and do not interact with cells or other important biological functions. The rise in antibiotic resistant bacteria can be attributed to the overuse and over-prescription of antibiotics and incorrect usage of antibiotics (for example prematurely stopping) [14]. These actions provide an evolutionary pressure on bacteria to mutate and gain resistance to the antibiotics. The phage therapy can contain any number of different phages that can target specific bacterial infections such as *Streptococcus pneumoniae* with minimal risk of side effects.

B.2.1 Current Applications: Bacterial Infection Control

One active area of research is the use of phages to control bacterial infections. Due to the specificity of phages, they can be used to target specific bacteria strains without affecting other beneficial bacteria. When sick with a bacterial infection, patients swallow antibiotic pills to help the body fight the infection. Antibiotics work by either interrupting intercellular processes like the synthesis of RNA [62], by disrupting the structural integrity of the cell wall [63], or by inhibiting protein synthesis [64].

However, antibiotics are not strain specific and indiscriminately kill gut and other bacteria. Common side effects of antibiotics, although usually not serious, include diarrhea, nausea, and headaches. It has also been shown that the effects of early-stage penicillin exposure in mice has found to have a long-lasting effect on the gut microbiome, frontal cortex gene expression, and amygdala gene expression [15]. Penicillin increases cytokine expression (small proteins used in cell signaling) in the frontal cortex of the brain, modifies the blood-brain barrier integrity, and alters behavior. The mice exhibited an increase in aggression and anxiety-like behavior [65]. Phages can be used as an alternative to antibiotics without the side effects and without affecting the gut biome.

With an increase in antibiotic usage, there has been an increase in antibiotic-resistant bacteria. The World Health Organization has stated that antibiotic resistance threatens the modern medicine and the sustainability of an effective, global public health response to the enduring threat from infectious diseases. Common infections, that previously

would have been easy to treat, are harder to treat, and can increase the risk of disease spread, severe illness, and death [66].

One area of research is exploring how bacteria can exchange traits such as phage resistance and antibiotic resistance. Some bacteria are multi-drug resistant, and don't react with the medicine anymore.

Laure and Ahn [16] showed evidence that *Salmonella Typhimurium* is more susceptible to ampicillin in the presence of phages, and phage-resistance can lead to reduced virulence and decreased antibiotic resistance.

Zhao et al. [17] showed that there exists an antagonist coevolution between the bacteria and phages, where the dynamics changed from an arms race dynamic (ARD) to a fluctuating selection dynamics (FSD). Due to phage selection and bacterial competition pressure, when the bacteria gained phage resistance, it lost antibiotic resistance. A genome analysis revealed mutations in the *btuB* gene of *Salmonella anatum*, with q higher mutation frequency in the ARD stage. A knockout experiment confirmed that the *btuB* gene is a receptor for the JNwz02 phage and resulted in reduced bacterial competitiveness. Further analysis detected multiple single nucleotide polymorphism (SNP) mutations in the phage-resistant strains. The SNPs potentially affected the membrane components, partially weakening the cell defense against antibiotics. These findings help advance our understanding of phage-host-antibiotics interactions and the impact of adaptations to antibiotic resistance. The research shows how phages can be used to reintroduce antibiotic susceptibility to previous insusceptible bacteria, preventing costly and lengthy research in new antibiotics [17].

Phage research is facing challenges due to bacterial strains evolving resistance to phages. Understanding the interplay between antibiotics and phages is essential for shaping future research [17].

B.3 Environmental Protection

Algae blooms, also called red tides, is the rapid spread of bacterial or algae organisms. Blooms are a growing environmental concern impacting water quality, aquatic ecosystems, and human health. These rapid increases in algae populations, often fueled by excess resources like nitrogen and phosphorus, can occur in freshwater, coastal, and marine environment.

Cyanobacteria blooms have major effects on the aquatic environment as well as human health. Cyanobacteria release nitrogen and phosphorous, which the bacteria use to grow

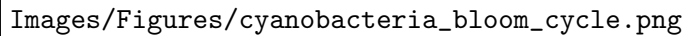


Figure B.3: Cyanobacteria degradation cycle, main hazards of cyanobacteria bloom to water bodies, aquatic organisms, and the human body. (DO: dissolved oxygen; SD: water transparency; Cond: conductivity; N: nitrogen; P: phosphorus; MCs: microcystins). [8]

with oxygen, outpacing other aquatic growth, and killing aquatic marine life. Bacterial toxins can make their way into the food and water consumed by humans, causing muscle fatigue, respiratory issues, liver damage, and gastrointestinal issues [8]. Figure B.3 shows the process of how cyanobacteria degrade and are absorbed into the environment, eventually making their way into the human body via various contact points.

B.3.1 Current Applications

There is interest in using phages to control cyanobacteria blooms. Phages can offer better and safer options than chemical options when trying to control bacterial blooms. Chemical options are indiscriminate, killing cyanobacteria, while also killing other beneficial bacteria and aquatic life, and can eventually seep into groundwater. Although not used to control bacteria blooms, some chemicals like PFAS, also called “Forever Chemicals”, can last a long time in the environment and don’t degrade and keep on negatively affecting the environment. Due to the specificity of phages, only the cyanobacteria will be targeted, and will not affect the surrounding environment.

Tucker and Pollard found that an isolated phage cocktail collected from Lake Baroon in Australia could decrease the abundance of *M. aeruginosa* by 95% within 6 days in a lab setting, before recovering within 3 weeks time [13].

There is evidence that phage-resistant bacteria can influence the population dynamics of other bacteria. It has been shown that the plankton level has been experimentally affected by the frequency of the phage-resistant *Nodularia* marine bacteria. Populations with high phage resistance (> 50%) dominate the plankton communities despite a high phage count and eventually out compete other bacteria due to their slower loss in population count. Contrastingly, populations of bacteria with low phage resistance (between 0% and 5%) were lysed to extinction, releasing resources like nitrogen. This

allows for other bacterial strains to absorb the resources and dominate the bacterial community. Phages and the lysis of bacterial strains can have a dramatic effect on community dynamics and composition of other entities like phages, bacteria, and resources [12]. Phages have the potential to be used as a highly specific strategy for the control of cyanobacterial blooms, with minimal effects to the environment, and offer control of bacterial blooms, with limited impact to the environment. Usage should be relatively safe, novel, efficient, and sensitive.

However, there are issues with using phages to control bacterial blooms. Bacterial blooms can cover vast areas, or be in areas that would be hard to reach like marshlands, applying phages to combat the bloom might be infeasible. If the method of choice was to spray a solution of water containing phages, the solution needs to be shipped to the site and loaded onto special boats to spray the solution into the water, or the trucks need to drive along the shore and spray the solution into the water.

The phage density in the solution will have to be relatively high to quickly combat the bloom. These problems provide major logistical problems with creating the phages in a lab or factory, transporting the phages, and finally the administration of the phages to the waterways. Phages can only diffuse through the water, and can't actively swim, so they are dependent on the rate of diffusion and water currents. This will be difficult in marshlands, where the bacteria can "hide" in the grass and crevices created by aquatic life. If the bloom is in a high current area, like in a river or a bay, the water can wash the phages away.

Scientists have not yet fully understood the phage infection mechanism, and research into the artificial engineering of phages is limited, making it challenging to conduct studies in this area [67, 68].

Algae can produce toxins that threaten wildlife, contaminate drinking water, and disrupt local economies dependent on fishing and tourism. In the state of Florida, between the years 1995 and 2000, the restaurant and hotel industry lost an estimated \$6.5 million to algae blooms. This accounts for about 25% of the average total monthly sales revenue in the region from June through October, the months that are most commonly affected by red tide[69]. During a red bloom event, hospital diagnoses in the county of Sarasota for pneumonia, gastrointestinal, and respiratory illness increased by 19%, 40% and 54% respectively [70, 71], with a respiratory illness visit costing between \$0.5 and \$4 million [72].

Appendix C

Appendix C: Flowchart of User and System Interactions

Figure C.1 shows how the user can interact with the system, the input and outputs for subsystems, and the systems working with one another. To read the flow chart, start from the top to the bottom. First the user creates a network using the GUI Network Creation Tool. After the graph is finished, the user provides an implementation of the network as an ODE model, using Python. Once finished, the user provides the network file and ODE model to the ODE solver. The solver uses information from the network file to determine the number of entities to create, parameter details (including names, values, and dimensions), and setting values. Then the user interacts with the Visualization Dashboard Tool, for example by clicking on buttons to run simulations, changing parameter values, (un)selecting checkboxes, and zooming in and out of plots, and hovering over plots to show data. Once a user has selected the parameter values, the parameter values are sent to the solver. The solver calculates the time and population values using the provided graph and ODE model and sends the data back to the Visualization Dashboard Tool, which then outputs the visualizations. If the user has run an ultimate analysis, then the user can query the saved data to make their own custom visualizations.



Figure C.1: The flowchart of user and system interactions. Read from top to bottom.

Appendix D

Appendix D: ODE Model Implementation

The code listed here is the implementation of Section 2.8.2.

Appendix E

Appendix E: Parameter Values Used

E.1 Realistic Growth Curves

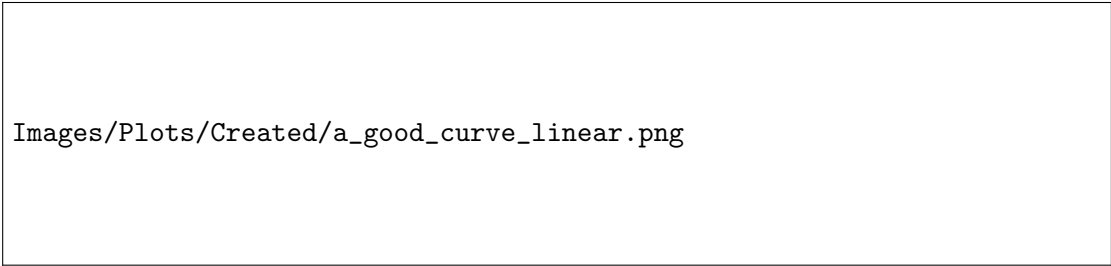
IC					
Resources	Uninfected Bacteria		Infected Bacteria		Phages
400	50		[0 0 0 0]		10
Vector Data					
τ	ω^i				
2.14	0				
Matrix Data					
e	v	K	r	β	
0.03	1.2	10	0.01	20	
Environment Data					
M	ω^o				
4	0				

Table E.1: The parameter values used for Figure 2.3.

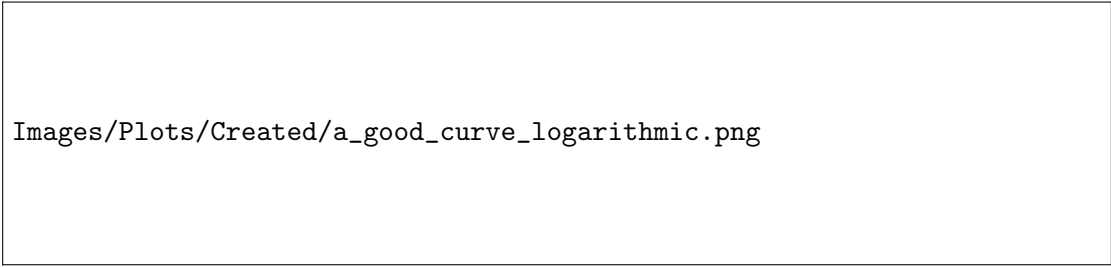
E.2 A Second Realistic Growth Curve

E.3 SOBOL Analysis

E.4 Complex Model



(a) A second realistic growth curve, linear y-axis



(b) A second realistic growth curve, logarithmic y-axis.

Figure E.1: The parameters used for this plot can be found in Table E.1.

IC					
Resources	Uninfected Bacteria		Infected Bacteria		Phages
200	50		[0 0 0 0]		10
Vector Data					
τ	ω^i				
0.7	0				
Matrix Data					
e	v	K	r	β	
0.12	1	10	0.001	10	
Environment Data					
M	ω^o				
4	0				

Table E.2: Another set of realistic growth curves. The linear and logarithmic plot of this data can be seen in Figure E.1

IC					
Resources	Uninfected Bacteria		Phages		
1-500	1-100		1-50		
Vector Data					
τ	ω^i				
0.5-3.5	0-100				
Matrix Data					
e	v	K	r	β	
0.05-0.25	0.8-1.9	10-250	0.001-0.2	1-100	
Environment Data					
ω^o					
0-0.1					
Other Data					
Seed Value	2nd Order	Number Samples		Simulations Run	Simulation Length
0	False	15		$2^{15}(9+2) = 360448$	15

Table E.3: The parameter values used for the SOBOL sensitivity analysis in Figure 4.1 (SOBOL analysis without washin and washout) and Figure F.1 (SOBOL analysis with washin and washout). For SOBOL analysis with washin and washout, there are $2^{15}(9+2) = 425984$ unique simulations run.

IC								
Resources			Uninfected Bacteria		Infected Bacteria		Phages	
[236 287 270]			[53 69]		$\begin{bmatrix} 0 & 0 & 0 & 0 \\ 0 & 0 & 0 & 0 \end{bmatrix}$		[10 5 8]	
Vector Data								
τ_b			ω_r^i					
[2.73340 2.25015]			[0 0 0]					
Matrix Data								
e_{br}			v_{br}					
$\begin{bmatrix} 0.15680 & 0.10871 & 0 \\ 0 & 0 & 0.18009 \end{bmatrix}$			$\begin{bmatrix} 1.27601 & 0.86393 & 0 \\ 0 & 0 & 1.22625 \end{bmatrix}$					
K_{br}			r_{pb}			β_{pb}		
$\begin{bmatrix} 139.58353 & 12.83058 & 0 \\ 0 & 0 & 82.86684 \end{bmatrix}$			$\begin{bmatrix} 0 & 0.11695 \\ 0.144459 & 0 \\ 0.11895 & 0.13065 \end{bmatrix}$			$\begin{bmatrix} 0 & 15 \\ 34 & 0 \\ 11 & 57 \end{bmatrix}$		
Environment Data								
M			ω^o					
4			0					

Table E.4: The parameter values used for the $3 \times 2 \times 3$ network model rounded to 5 decimal points. If there is no edge between a phage, bacteria, or resource, then in the matrix representation of the parameter, 0 is stored as the default value.

Appendix F

Appendix F: Extra Plots and Figures

F.1 SOBOL Analysis With Washin and Washout

F.1.1 Final Value Analysis

F.1.1.1 Resources

Despite the resource consumption rate directly depending on e, v and K , the parameters had very little influence on the final value as evidence by the ST and S1 bar being near 0. The resource population was mainly driven by the washin and washout value. The peak resources are driven completely by the washin rate. Not many interactions between two or more parameters were occurring.

F.1.1.2 Phages

The most important factor for the final phage value is r , followed by β and ω^o . The other parameters had little to no effect on the final phage value.

F.1.1.3 Total Bacteria

The sum of uninfected and infected bacteria depended heavily on higher order interactions as $ST_i \gg S1_i$. Although not shown, the bar plots for the total bacteria resembled that of the bar-plots for the uninfected bacteria, and less that of the infected bacteria.

F.1.2 Peak Value and Time of peak

To create the custom SOBOL analyses, the peak value and the time at the peak of the population is measured and analyzed. The peak is defined as the point where the population reaches 95% of its absolute maximum value. The time at peak is measured at the point in time that the population reaches 95% of the maximum value. This removes unintended side effects of the simulation. For populations that are only increasing in value, this prevents the measured peak from bunching up at the end of the simulation, skewing the data. As the peak is defined at 95% of the absolute maximum value, populations that have a faster increase on population count at the end will have a time value closer towards the end of the simulation. For populations that reach a plateau, the 95% rule will push the peak time towards the beginning of the simulation, while still “respecting” the absolute final value since $95\% \approx 100\%$. The 95% rule can fail under certain situations, such as when there is cyclic behavior. See Appendix F.2 for a more detailed explanation on why the 95% rule is used.

The results of the SOBOL peak and time at peak analyses can be seen in Figure F.1b and Figure F.1c. Although some of the bars between the final, peak, and time at peak values are the same, some are different. But overall, similar values can be seen across the the final, peak, and time at peak analyses. The peak infected values are more certain compared to the final infected values, which could be due to the 95% rule removing some of the noise of the simulation. The time at peak values have less error compared to the final and peak value. This is due to the restricted range of values. The time at peak value can only fall somewhere between 0 and 15, the start and end values of the simulation respectively. The final and peak values can fall anywhere between 0 and any value, depending on the IC and how high the population can rise, and how fast the population can fall, *if* the population count falls.

F.2 Why 95%?

The 95% rule helps in the IVA analysis. Due to the solver, when taking the absolute peak value, the same time value can occur. Or in an ever increasing value like phages, the peak values occur at the last time step of the simulation, or plateaus and doesn't grow anymore. However, as the parameter value is changing, each graph for every input change will change the growth rate of the entity, changing how fast the entity population grows.

Figure F.2 shows how using the 95% rule vs the 100% rule for finding the max value reached helps smooth out computational errors from the ODE solver and smooths out



Figure F.1: SOBOL analyses for the final, peak, and time of peak value with a washin and washout rate. The data was saved from the dashboard and plotted using Matplotlib. The values used for this SOBOL test can be found in Table E.3.

the shape. For the phages, using the 100% rule (Figure F.2b) shows that the population peaked at the end of the simulation, $t = 15$, for all e values. However at $t = 15$, the population plateaued, as evident by the line graph. Plotting the same plot, but calculating the peak at 95% of the actual peak (Figure F.2a) shows that the green line ($e = 0.25$) “reached” its peak at $t = 8.4$ before the red line ($e = 0.05$) at $t = 9.4$, a full unit of time after $e = 0.25$. The user can thus conclude that for this instance, larger e values will cause the phage population to reach its “peak” faster than smaller e values.

Figure F.2c and Figure F.2d likewise show how the 95% rule can improve analysis of the change in peak time. Figure F.2d shows how apparently the peak is reached at set time values. Due to how *solve_ivp()* from SciPy works, it automatically chooses time values that it thinks would best capture the dynamics of the system without calculating too many steps. The user can control the step size by decreasing the absolute and relative error bounds, as well as by minimizing the time steps. The user can also provide their own time range with the number of steps to run, increasing the control of the time values chosen. It takes about 0.02321 seconds to run a simulation for 15 time units, where 200 time steps are selected and solved by the solver. Comparatively, a simulation with 1000 time units and 1000000 (a 5000x increase in samples) equidistant time samples takes about 1.71651 seconds to run, a 73.95562258x increase in time spent computing the simulation. The total time taken to run the whole method call, a call to the simple graph maker at the top of the dashboard took 1.76130 seconds vs 17.70634 seconds.

Alternatively instead of controlling the solver, the user can use the 95% rule. Although some accuracy is lost. Going from the 100% rule to the 95% rule, the solver still captures the peak values and the dynamics, but the accuracy is lost. The 100% rule shows that for $e = 0.25$, the time the uninfected population reached its peak occurred at $t = 3.2$.

But for the 95% rule, the time at which the peak occurred at is at $t = 3.05$. The slope (the a value) and the intercept (the c value) are somewhat similar, with very high and similar R^2 values (0.97), suggesting a good linear fit of the data.

Figure F.2e shows how the by increasing the time sampling to more fine grained results in a more accurate graph. Instead of having the solver choose the time values to test, 1000 equidistant time values were selected between 0 and 15. The solver can more accurately calculate the population values and calculate the proper peak time. Comparing the 100% rule without the custom time values with the 100% rule with the custom time values shows the same time values were calculated. in both, the $e = 0.25$ resulted in a time of peak at 3.2 and for $e = 0.05$, the time of peak occurred at $t = 3.95$. This is in stark comparison to the 95% rule vs 100% rule without the custom time, showing a difference of 0.15 time units. The custom time values also preserved the shape of the curve e -value vs time curve, being almost identical to that of the 95% rule as seen in Figure F.2c and Figure F.2e.

Another issue that arises with the custom time is that it doesn't solve the issue seen with the phages, where the time of peak is at $t = 15$.

The user can control the % rule with a value input on the dashboard. They can select to use the 95% rule, or 100% rule, or even 83% rule if they want by changing the value they use. The user can use their own custom time values, to ensure that they get high quality curves.

F.3 Varying r and β In A $3 \times 2 \times 3$ System

Figure F.3, Figure F.4, and Figure F.5 show a 7x7 matrix of figures, each with a unique parameter set. In each sub-figure, the values of r and β are varied as follows: $r = 0.5, 1.1, 1.7, 2.3, 2.9, 3.5, \text{inf}$; $\beta = 0, 20, 40, 60, 80, 100, \text{inf}$. "inf" in the figures, represented as *np.inf* in the code, the representation of ∞ , represents the original parameter values used in the IC, vector data, or matrix data. Each figure shows the effect of varying the washout rate, with values set to 0, 0.02, and 0.05, respectively. All initial phage values were set to 10. This was done to really show how the different interactions with the bacteria, and the value of the parameters affected the phage growth. The default values for the parameters can be found in Table E.4.

Images/Plots/Created/IVA/initial_value_analysis_Phages_95.png

(a) IVA for phage population, 95% rule

Images/Plots/Created/IVA/initial_value_analysis_Phages_100.png

(b) IVA for phage population, 100% rule.

Images/Plots/Created/IVA/initial_value_analysis_Uninfected_Bacteria_95.png

(c) IVA for uninfected population, 95% rule.

Images/Plots/Created/IVA/initial_value_analysis_Uninfected_Bacteria_100.png

(d) IVA for uninfected population, 100% rule.

Images/Plots/Created/IVA/initial_value_analysis_Uninfected_Bacteria_100_own_time.png

(e) IVA for uninfected population, 100% rule, 1000 equidistant time steps.

Figure F.2: Testing the 95% rule vs the 100% rule, where the time at the absolute peak is taken and plotted in the second plot. A comparison of phages and uninfected bacteria is shown. Verification of the graph shape between the 95% rule graph and a frequent time step with 100% rule can be seen between c) and e). The ϵ value is changed, ranging from 0.05 to 0.25.

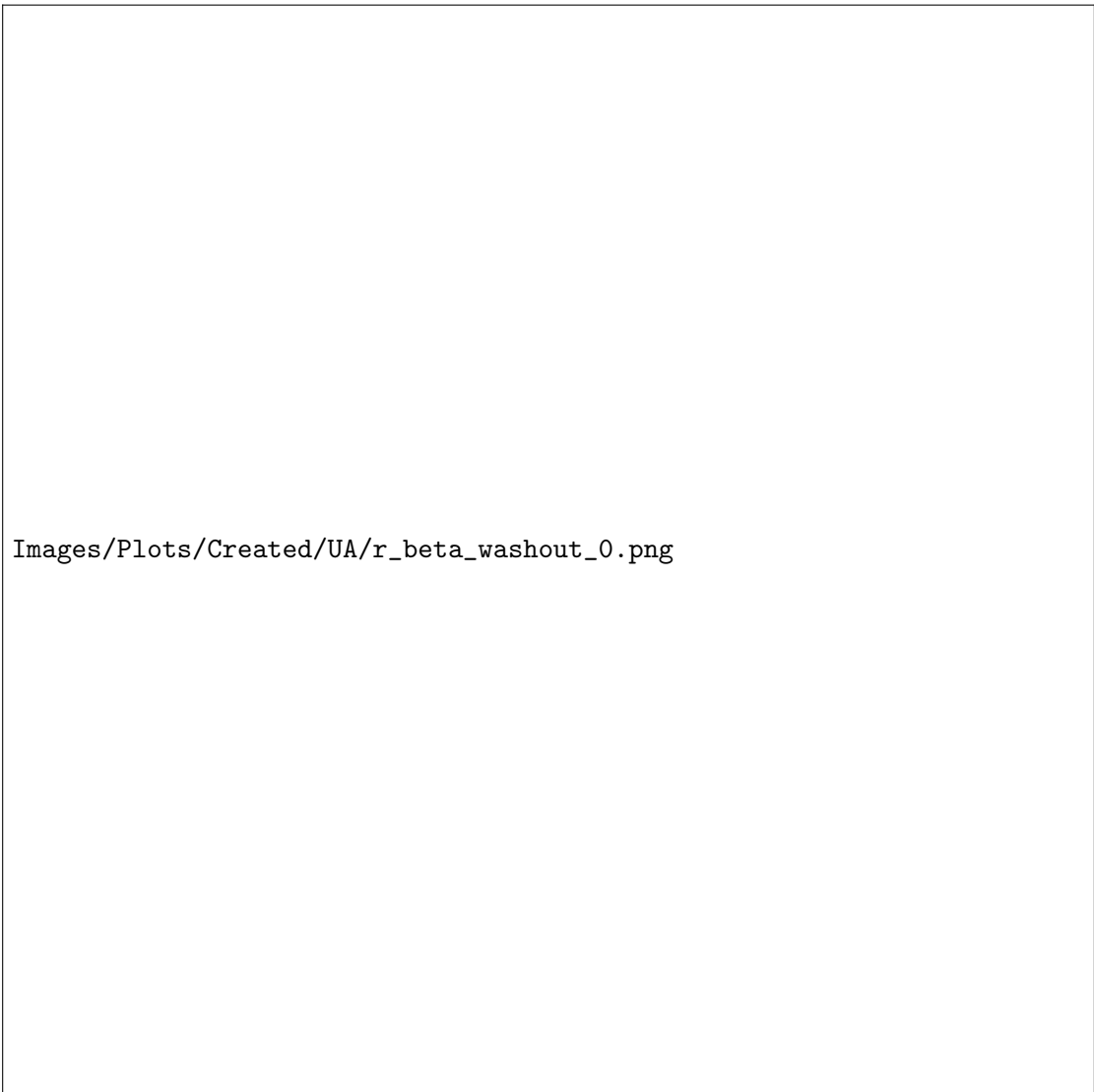


Figure F.3: Washout $\omega^o = 0$.

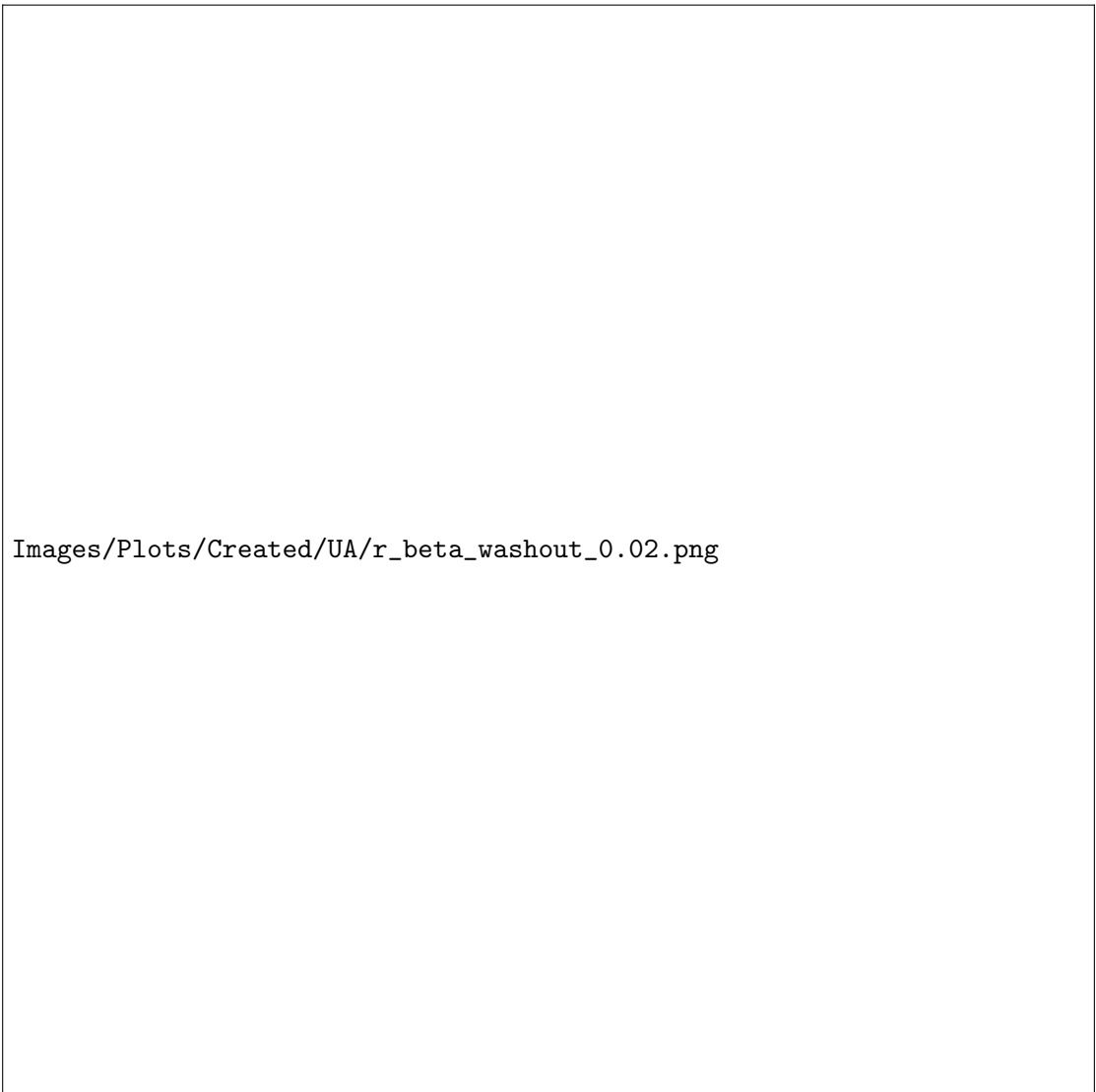


Figure F.4: Washout $\omega^o = 0.02$.

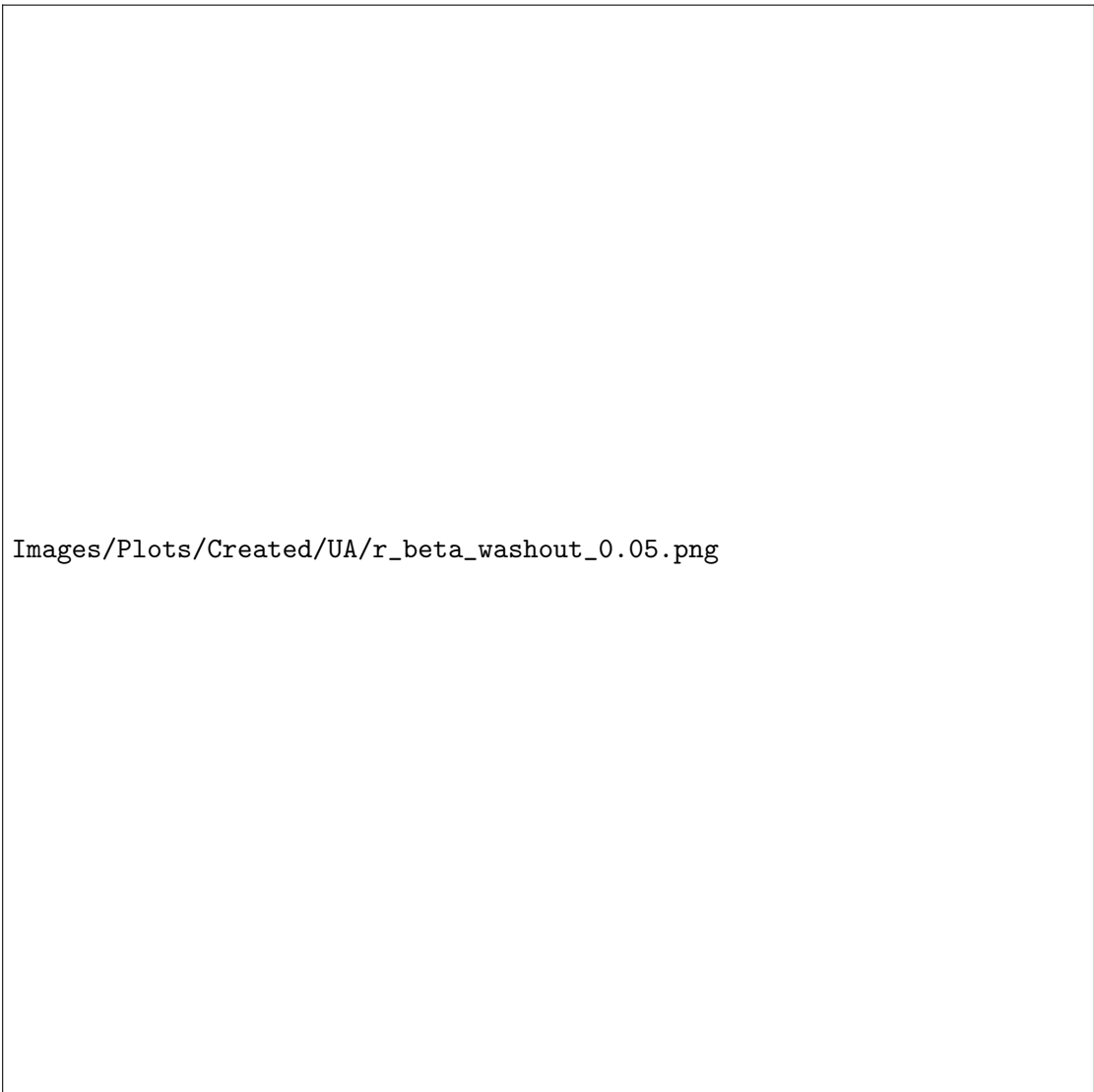


Figure F.5: Washout $\omega^o = 0.05$.

Bibliography

- [1] Yuncong Geng, Thu Vu Phuc Nguyen, Ehsan Homaei, and Ido Golding. Using bacterial population dynamics to count phages and their lysogens. *Nature Communications*, 15(1):7814, September 2024. ISSN 2041-1723. doi: 10.1038/s41467-024-51913-6. URL <https://www.nature.com/articles/s41467-024-51913-6>.
- [2] Allan Campbell. The future of bacteriophage biology. *Nature Reviews Genetics*, 4(6):471–477, June 2003. ISSN 1471-0056, 1471-0064. doi: 10.1038/nrg1089. URL <https://www.nature.com/articles/nrg1089>.
- [3] Naomi Iris van den Berg, Daniel Machado, Sophia Santos, Isabel Rocha, Jeremy Chacón, William Harcombe, Sara Mitri, and Kiran R. Patil. Ecological modelling approaches for predicting emergent properties in microbial communities. *Nature Ecology & Evolution*, 6(7):855–865, July 2022. ISSN 2397-334X. doi: 10.1038/s41559-022-01746-7. URL <https://www.nature.com/articles/s41559-022-01746-7>.
- [4] Anders S. Nilsson. Cocktail, a Computer Program for Modelling Bacteriophage Infection Kinetics. *Viruses*, 14(11):2483, November 2022. ISSN 1999-4915. doi: 10.3390/v14112483. URL <https://www.mdpi.com/1999-4915/14/11/2483>.
- [5] Konrad Krysiak-Baltyn, Gregory J. O. Martin, Anthony D. Stickland, Peter J. Scales, and Sally L. Gras. Simulation of phage dynamics in multi-reactor models of complex wastewater treatment systems. *Biochemical Engineering Journal*, 122: 91–102, June 2017. ISSN 1369-703X. doi: 10.1016/j.bej.2016.10.011. URL <https://www.sciencedirect.com/science/article/pii/S1369703X16302728>.
- [6] Nitzan Soffer, Tamar Abuladze, Joelle Woolston, Manrong Li, Leigh Farris Hanna, Serena Heyse, Duane Charbonneau, and Alexander Sulakvelidze. Bacteriophages safely reduce Salmonella contamination in pet food and raw pet food ingredients. *Bacteriophage*, 6(3):e1220347, July 2016. ISSN null. doi: 10.1080/21597081.2016.1220347. URL <https://doi.org/10.1080/21597081.2016.1220347>.
- [7] Xuan Zhang, Yan Dong Niu, Yuchen Nan, Kim Stanford, Rick Holley, Tim McAllister, and Claudia Narváez-Bravo. SalmoFresh™ effectiveness in controlling

- Salmonella on romaine lettuce, mung bean sprouts and seeds. *International Journal of Food Microbiology*, 305:108250, September 2019. ISSN 0168-1605. doi: 10.1016/j.ijfoodmicro.2019.108250. URL <https://www.sciencedirect.com/science/article/pii/S0168160519301709>.
- [8] Weizhen Zhang, Jing Liu, Yunxing Xiao, Yumiao Zhang, Yangjinzhi Yu, Zheng Zheng, Yafeng Liu, and Qi Li. The Impact of Cyanobacteria Blooms on the Aquatic Environment and Human Health. *Toxins*, 14(10):658, September 2022. ISSN 2072-6651. doi: 10.3390/toxins14100658. URL <https://www.ncbi.nlm.nih.gov/pmc/articles/PMC9611879/>.
- [9] Basem Al-Shayeb, Rohan Sachdeva, Lin-Xing Chen, Fred Ward, Patrick Munk, Audra Devoto, Cindy J. Castelle, Matthew R. Olm, Keith Bouma-Gregson, Yuki Amano, Christine He, Raphaël Méheust, Brandon Brooks, Alex Thomas, Adi Lavy, Paula Matheus-Carnevali, Christine Sun, Daniela S. A. Goltsman, Mikayla A. Borton, Allison Sharrar, Alexander L. Jaffe, Tara C. Nelson, Rose Kantor, Ray Keren, Katherine R. Lane, Ibrahim F. Farag, Shufei Lei, Kari Finstad, Ronald Amundson, Karthik Anantharaman, Jinglie Zhou, Alexander J. Probst, Mary E. Power, Susannah G. Tringe, Wen-Jun Li, Kelly Wrighton, Sue Harrison, Michael Morowitz, David A. Relman, Jennifer A. Doudna, Anne-Catherine Lehours, Lesley Warren, Jamie H. D. Cate, Joanne M. Santini, and Jillian F. Banfield. Clades of huge phages from across Earth’s ecosystems. *Nature*, 578(7795):425–431, February 2020. ISSN 1476-4687. doi: 10.1038/s41586-020-2007-4. URL <https://www.nature.com/articles/s41586-020-2007-4>.
- [10] Teagan L Brown, Oliver J Charity, and Evelien M Adriaenssens. Ecological and functional roles of bacteriophages in contrasting environments: Marine, terrestrial and human gut. *Current Opinion in Microbiology*, 70:102229, December 2022. ISSN 1369-5274. doi: 10.1016/j.mib.2022.102229. URL <https://www.sciencedirect.com/science/article/pii/S1369527422001138>.
- [11] Sandra Chibani-Chennoufi, Anne Bruttin, Marie-Lise Dillmann, and Harald Brüssow. Phage-Host Interaction: An Ecological Perspective. *Journal of Bacteriology*, 186(12):3677–3686, June 2004. ISSN 0021-9193. doi: 10.1128/JB.186.12.3677-3686.2004. URL <https://www.ncbi.nlm.nih.gov/pmc/articles/PMC419959/>.
- [12] Sebastián Coloma, Ursula Gaedke, Kaarina Sivonen, and Teppo Hiltunen. Frequency of virus-resistant hosts determines experimental community dynamics. *Ecology*, 100(1):e02554, 2019. ISSN 1939-9170. doi: 10.1002/ecy.2554. URL <https://onlinelibrary.wiley.com/doi/abs/10.1002/ecy.2554>.

- [13] Stephen Tucker and Peter Pollard. Identification of Cyanophage Ma-LBP and Infection of the Cyanobacterium *Microcystis aeruginosa* from an Australian Subtropical Lake by the Virus. *Applied and Environmental Microbiology*, 71(2):629–635, February 2005. doi: 10.1128/AEM.71.2.629-635.2005. URL <https://journals.asm.org/doi/10.1128/aem.71.2.629-635.2005>.
- [14] Stephen Odonkor and Kennedy Addo. Bacteria Resistance to Antibiotics: Recent Trends and Challenges. *International Journal of Biological & Medical Research*, pages 1204–1210, January 2011.
- [15] Angelina Volkova, Kelly Ruggles, Anjelique Schulfer, Zhan Gao, Stephen D. Ginsberg, and Martin J. Blaser. Effects of early-life penicillin exposure on the gut microbiome and frontal cortex and amygdala gene expression. *iScience*, 24(7):102797, July 2021. ISSN 2589-0042. doi: 10.1016/j.isci.2021.102797. URL <https://www.ncbi.nlm.nih.gov/pmc/articles/PMC8324854/>.
- [16] Nana Nguefang Laure and Juhee Ahn. Phage resistance-mediated trade-offs with antibiotic resistance in *Salmonella Typhimurium*. *Microbial Pathogenesis*, 171:105732, October 2022. ISSN 08824010. doi: 10.1016/j.micpath.2022.105732. URL <https://linkinghub.elsevier.com/retrieve/pii/S088240102200345X>.
- [17] Yuanyang Zhao, Mei Shu, Ling Zhang, Chan Zhong, Ningbo Liao, and Guoping Wu. Phage-driven coevolution reveals trade-off between antibiotic and phage resistance in *Salmonella anatum*. *ISME Communications*, 4(1):ycae039, January 2024. ISSN 2730-6151. doi: 10.1093/ismeco/ycae039. URL <https://doi.org/10.1093/ismeco/ycae039>.
- [18] Beata Kowalska. Fresh vegetables and fruit as a source of *Salmonella* bacteria. *Annals of agricultural and environmental medicine: AAEM*, 30(1):9–14, March 2023. ISSN 1898-2263. doi: 10.26444/aaem/156765.
- [19] Edel Stone, Katrina Campbell, Irene Grant, and Olivia McAuliffe. Understanding and Exploiting Phage–Host Interactions. *Viruses*, 11(6):567, June 2019. ISSN 1999-4915. doi: 10.3390/v11060567. URL <https://www.ncbi.nlm.nih.gov/pmc/articles/PMC6630733/>.
- [20] Dalton V. Banh, Cameron G. Roberts, Adrian Morales-Amador, Brandon A. Berryhill, Waqas Chaudhry, Bruce R. Levin, Sean F. Brady, and Luciano A. Marraffini. Bacterial cGAS senses a viral RNA to initiate immunity. *Nature*, 623(7989):1001–1008, November 2023. ISSN 1476-4687. doi: 10.1038/s41586-023-06743-9. URL <https://www.nature.com/articles/s41586-023-06743-9>.

- [21] Asaf Levy, Moran G. Goren, Ido Yosef, Oren Auster, Miriam Manor, Gil Amitai, Rotem Edgar, Udi Qimron, and Rotem Sorek. CRISPR adaptation biases explain preference for acquisition of foreign DNA. *Nature*, 520(7548):505–510, April 2015. ISSN 1476-4687. doi: 10.1038/nature14302. URL <https://www.nature.com/articles/nature14302>.
- [22] Joanna Warwick-Dugdale, Holger H. Buchholz, Michael J. Allen, and Ben Temperton. Host-hijacking and planktonic piracy: How phages command the microbial high seas. *Virology Journal*, 16(1):1–13, December 2019. ISSN 1743-422X. doi: 10.1186/s12985-019-1120-1. URL <https://virologyj.biomedcentral.com/articles/10.1186/s12985-019-1120-1>.
- [23] P. M. Sharp. Molecular evolution of bacteriophages: Evidence of selection against the recognition sites of host restriction enzymes. *Molecular Biology and Evolution*, 3(1):75–83, January 1986. ISSN 0737-4038. doi: 10.1093/oxfordjournals.molbev.a040377.
- [24] Matthew K Waldor and David I Friedman. Phage regulatory circuits and virulence gene expression. *Current Opinion in Microbiology*, 8(4):459–465, August 2005. ISSN 1369-5274. doi: 10.1016/j.mib.2005.06.001. URL <https://www.sciencedirect.com/science/article/pii/S1369527405000755>.
- [25] Louis-Charles Fortier and Ognjen Sekulovic. Importance of prophages to evolution and virulence of bacterial pathogens. *Virulence*, 4(5):354–365, July 2013. ISSN 2150-5594. doi: 10.4161/viru.24498. URL <https://www.ncbi.nlm.nih.gov/pmc/articles/PMC3714127/>.
- [26] Anastasia A. Aksyuk and Michael G. Rossmann. Bacteriophage Assembly. *Viruses*, 3(3):172–203, February 2011. ISSN 1999-4915. doi: 10.3390/v3030172. URL <https://www.ncbi.nlm.nih.gov/pmc/articles/PMC3185693/>.
- [27] I. N. Wang, D. L. Smith, and R. Young. Holins: The protein clocks of bacteriophage infections. *Annual Review of Microbiology*, 54:799–825, 2000. ISSN 0066-4227. doi: 10.1146/annurev.micro.54.1.799.
- [28] Richard E Lenski. TWO-STEP RESISTANCE BY ESCHERICHIA COLI B TO BACTERIOPHAGE T2. *Genetics*, 107(1):1–7, May 1984. ISSN 1943-2631. doi: 10.1093/genetics/107.1.1. URL <https://doi.org/10.1093/genetics/107.1.1>.
- [29] Laith Harb, Karthik Chamakura, Pratick Khara, Peter J. Christie, Ry Young, and Lanying Zeng. ssRNA phage penetration triggers detachment of the F-pilus. *Proceedings of the National Academy of Sciences of the United States of America*, 117

- (41):25751–25758, October 2020. ISSN 0027-8424. doi: 10.1073/pnas.2011901117. URL <https://www.ncbi.nlm.nih.gov/pmc/articles/PMC7568308/>.
- [30] Sanju Tamang. Horizontal Gene Transfer in Prokaryotes and Eukaryotes, September 2023. URL <https://microbenotes.com/horizontal-gene-transfer-prokaryotes-eukaryotes/>.
- [31] Laura M. Kasman and La Donna Porter. Bacteriophages. In *StatPearls*. StatPearls Publishing, Treasure Island (FL), 2025. URL <http://www.ncbi.nlm.nih.gov/books/NBK493185/>.
- [32] Demeng Tan, Sine Lo Svenningsen, and Mathias Middelboe. Quorum Sensing Determines the Choice of Antiphage Defense Strategy in *Vibrio anguillarum*. *mBio*, 6(3):10.1128/mbio.00627–15, June 2015. doi: 10.1128/mbio.00627-15. URL <https://journals.asm.org/doi/10.1128/mbio.00627-15>.
- [33] Avinoam Rabinovitch, Ira Aviram, and Arie Zaritsky. Bacterial debris—an ecological mechanism for coexistence of bacteria and their viruses. *Journal of Theoretical Biology*, 224(3):377–383, October 2003. ISSN 0022-5193. doi: 10.1016/S0022-5193(03)00174-7. URL <https://www.sciencedirect.com/science/article/pii/S0022519303001747>.
- [34] James J. Bull, Kelly A. Christensen, Carly Scott, Benjamin R. Jack, Cameron J. Crandall, and Stephen M. Krone. Phage-Bacterial Dynamics with Spatial Structure: Self Organization around Phage Sinks Can Promote Increased Cell Densities. *Antibiotics*, 7(1):8, March 2018. ISSN 2079-6382. doi: 10.3390/antibiotics7010008. URL <https://www.mdpi.com/2079-6382/7/1/8>.
- [35] Anika Gupta, Norma Morella, Dmitry Sutormin, Naisi Li, Karl Gaisser, Alexander Robertson, Yaroslav Ispolatov, Georg Seelig, Neelendu Dey, and Anna Kuchina. Combinatorial phenotypic landscape enables bacterial resistance to phage infection, January 2025. URL <https://www.biorxiv.org/content/10.1101/2025.01.13.632860v1>.
- [36] Stephen T. Abedon. Phage “delay” towards enhancing bacterial escape from biofilms: A more comprehensive way of viewing resistance to bacteriophages. *AIMS Microbiology*, 3(microbiol-03-00186):186–226, 2017. ISSN 2471-1888. doi: 10.3934/microbiol.2017.2.186. URL <http://www.aimspress.com/article/doi/10.3934/microbiol.2017.2.186>.
- [37] Rasmus Skytte Eriksen, Sine L. Svenningsen, Kim Sneppen, and Namiko Mitarai. A growing microcolony can survive and support persistent propagation of virulent phages. *Proceedings of the National Academy of Sciences*, 115(2):337–342, January

2018. ISSN 0027-8424, 1091-6490. doi: 10.1073/pnas.1708954115. URL <https://pnas.org/doi/full/10.1073/pnas.1708954115>.
- [38] Christoph Lohrmann, Christian Holm, and Sujit S. Datta. Influence of bacterial swimming and hydrodynamics on attachment of phages. *Soft Matter*, 20(24):4795–4805, June 2024. ISSN 1744-6848. doi: 10.1039/D4SM00060A. URL <https://pubs.rsc.org/en/content/articlelanding/2024/sm/d4sm00060a>.
- [39] Pramalkumar H. Patel, Véronique L. Taylor, Chi Zhang, Landon J. Getz, Alexa D. Fitzpatrick, Alan R. Davidson, and Karen L. Maxwell. Anti-phage defence through inhibition of virion assembly. *Nature Communications*, 15(1):1644, February 2024. ISSN 2041-1723. doi: 10.1038/s41467-024-45892-x. URL <https://www.nature.com/articles/s41467-024-45892-x>.
- [40] Michael J. Bucher and Daniel M. Czyż. Phage against the Machine: The SIE-ence of Superinfection Exclusion. *Viruses*, 16(9):1348, August 2024. ISSN 1999-4915. doi: 10.3390/v16091348.
- [41] Shuji Kanamaru, Kazuya Uchida, Mai Nemoto, Alec Fraser, Fumio Arisaka, and Petr G. Leiman. Structure and Function of the T4 Spackle Protein Gp61.3. *Viruses*, 12(10):1070, September 2020. ISSN 1999-4915. doi: 10.3390/v12101070. URL <https://www.ncbi.nlm.nih.gov/pmc/articles/PMC7650644/>.
- [42] Justin C. Leavitt, Brianna M. Woodbury, Eddie B. Gilcrease, Charles M. Bridges, Carolyn M. Teschke, and Sherwood R. Casjens. Bacteriophage P22 SieA-mediated superinfection exclusion. *mBio*, 15(2):e02169–23, January 2024. doi: 10.1128/mbio.02169-23. URL <https://journals.asm.org/doi/10.1128/mbio.02169-23>.
- [43] Yuval Mulla, Janina Müller, Denny Trimcev, and Tobias Bollenbach. Extreme diversity of phage amplification rates and phage-antibiotic interactions revealed by PHORCE, December 2024. URL <https://www.biorxiv.org/content/10.1101/2024.06.07.597930v3>.
- [44] Jacob Beal, Natalie G. Farny, Traci Haddock-Angelli, Vinoo Selvarajah, Geoff S. Baldwin, Russell Buckley-Taylor, Markus Gershater, Daisuke Kiga, John Marken, Vishal Sanchania, Abigail Sison, and Christopher T. Workman. Robust estimation of bacterial cell count from optical density. *Communications Biology*, 3(1):512, September 2020. ISSN 2399-3642. doi: 10.1038/s42003-020-01127-5. URL <https://www.nature.com/articles/s42003-020-01127-5>.
- [45] Portia Mira, Pamela Yeh, and Barry G. Hall. Estimating microbial population data from optical density. *PLOS ONE*, 17(10):e0276040, October 2022. ISSN 1932-6203.

- doi: 10.1371/journal.pone.0276040. URL <https://journals.plos.org/plosone/article?id=10.1371/journal.pone.0276040>.
- [46] Advanced Wastewater Modelling | GPS-X - Hydromantis. URL <https://www.hydromantis.com/GPSX-innovative.html>.
- [47] Jacqueline Heard, Emma Harvey, Bruce B. Johnson, John D. Wells, and Michael J. Angove. The effect of filamentous bacteria on foam production and stability. *Colloids and Surfaces. B, Biointerfaces*, 63(1):21–26, May 2008. ISSN 0927-7765. doi: 10.1016/j.colsurfb.2007.10.011.
- [48] Brendan J. M. Bohannon and Richard E. Lenski. Effect of Resource Enrichment on a Chemostat Community of Bacteria and Bacteriophage. *Ecology*, 78(8):2303–2315, 1997. ISSN 1939-9170. doi: 10.1890/0012-9658(1997)078[2303:EOREOA]2.0.CO;2. URL <https://onlinelibrary.wiley.com/doi/abs/10.1890/0012-9658%281997%29078%5B2303%3AEOREOA%5D2.0.CO%3B2>.
- [49] Richard E. Lenski. Dynamics of Interactions between Bacteria and Virulent Bacteriophage. In K. C. Marshall, editor, *Advances in Microbial Ecology*, pages 1–44. Springer US, Boston, MA, 1988. ISBN 978-1-4684-5409-3. doi: 10.1007/978-1-4684-5409-3_1. URL https://doi.org/10.1007/978-1-4684-5409-3_1.
- [50] Pauli Virtanen, Ralf Gommers, Travis E. Oliphant, Matt Haberland, Tyler Reddy, David Cournapeau, Evgeni Burovski, Pearu Peterson, Warren Weckesser, Jonathan Bright, Stéfan J. van der Walt, Matthew Brett, Joshua Wilson, K. Jarrod Millman, Nikolay Mayorov, Andrew R. J. Nelson, Eric Jones, Robert Kern, Eric Larson, C. J. Carey, İlhan Polat, Yu Feng, Eric W. Moore, Jake VanderPlas, Denis Laxalde, Josef Perktold, Robert Cimrman, Ian Henriksen, E. A. Quintero, Charles R. Harris, Anne M. Archibald, Antônio H. Ribeiro, Fabian Pedregosa, and Paul van Mulbregt. SciPy 1.0: Fundamental algorithms for scientific computing in Python. *Nature Methods*, 17(3):261–272, March 2020. ISSN 1548-7105. doi: 10.1038/s41592-019-0686-2. URL <https://www.nature.com/articles/s41592-019-0686-2>.
- [51] J. R. Dormand and P. J. Prince. A family of embedded Runge-Kutta formulae. *Journal of Computational and Applied Mathematics*, 6(1):19–26, March 1980. ISSN 0377-0427. doi: 10.1016/0771-050X(80)90013-3. URL <https://www.sciencedirect.com/science/article/pii/0771050X80900133>.
- [52] Dash Documentation & User Guide | Plotly. URL <https://dash.plotly.com/>.

- [53] I. M Sobol'. Global sensitivity indices for nonlinear mathematical models and their Monte Carlo estimates. *Mathematics and Computers in Simulation*, 55(1):271–280, February 2001. ISSN 0378-4754. doi: 10.1016/S0378-4754(00)00270-6. URL <https://www.sciencedirect.com/science/article/pii/S0378475400002706>.
- [54] Python Software Foundation. Python programming language, version 3.11.6, 2024. URL <https://www.python.org>. Accessed: 2025-05-19.
- [55] Charles R. Harris, K. Jarrod Millman, Stéfan J. van der Walt, Ralf Gommers, Pauli Virtanen, David Cournapeau, Eric Wieser, Julian Taylor, Sebastian Berg, Nathaniel J. Smith, Robert Kern, Matti Picus, Stephan Hoyer, Marten H. van Kerkwijk, Matthew Brett, Allan Haldane, Jaime Fernández del Río, Mark Wiebe, Pearu Peterson, Pierre Gérard-Marchant, Kevin Sheppard, Tyler Reddy, Warren Weckesser, Hameer Abbasi, Christoph Gohlke, and Travis E. Oliphant. Array programming with NumPy. *Nature*, 585(7825):357–362, September 2020. doi: 10.1038/s41586-020-2649-2. URL <https://doi.org/10.1038/s41586-020-2649-2>.
- [56] Takuya Iwanaga, William Usher, and Jonathan Herman. Toward SALib 2.0: Advancing the accessibility and interpretability of global sensitivity analyses. *Socio-Environmental Systems Modelling*, 4:18155–18155, May 2022. ISSN 2663-3027. doi: 10.18174/sesmo.18155. URL <https://sesmo.org/article/view/18155>.
- [57] Jon Herman and Will Usher. SALib: An open-source Python library for Sensitivity Analysis. *Journal of Open Source Software*, 2(9):97, January 2017. ISSN 2475-9066. doi: 10.21105/joss.00097. URL <https://joss.theoj.org/papers/10.21105/joss.00097>.
- [58] Aric Hagberg, Pieter J. Swart, and Daniel A. Schult. Exploring network structure, dynamics, and function using NetworkX. Technical Report LA-UR-08-05495; LA-UR-08-5495, Los Alamos National Laboratory (LANL), Los Alamos, NM (United States), January 2008. URL <https://www.osti.gov/biblio/960616>.
- [59] J. D. Hunter. Matplotlib: A 2d graphics environment. *Computing in Science & Engineering*, 9(3):90–95, 2007. doi: 10.1109/MCSE.2007.55.
- [60] Raunak Dey, Ashley R. Coenen, Natalie E. Solonenko, Marie N. Burris, Anna I. Mackey, Julia Galasso, Christine L. Sun, David Demory, Daniel Muratore, Stephen J. Beckett, Matthew B. Sullivan, and Joshua S. Weitz. Emergent higher-order interactions enable coexistence in phage-bacteria community dynamics, May 2025. URL <https://www.biorxiv.org/content/10.1101/2025.05.15.651590v1>.

- [61] Lars Fieseler and Steven Hagens. Food Safety. In David R. Harper, Stephen T. Abedon, Benjamin H. Burrowes, and Malcolm L. McConville, editors, *Bacteriophages: Biology, Technology, Therapy*, pages 857–890. Springer International Publishing, Cham, 2021. ISBN 978-3-319-41986-2. doi: 10.1007/978-3-319-41986-2_29. URL https://doi.org/10.1007/978-3-319-41986-2_29.
- [62] Heinz G. Floss and Tin-Wein Yu. Rifamycin Mode of Action, Resistance, and Biosynthesis. *Chemical Reviews*, 105(2):621–632, February 2005. ISSN 0009-2665. doi: 10.1021/cr030112j. URL <https://doi.org/10.1021/cr030112j>.
- [63] A. Tomasz. The Mechanism of the Irreversible Antimicrobial Effects of Penicillins: How the Beta-Lactam Antibiotics Kill and Lyse Bacteria. *Annual Review of Microbiology*, 33(Volume 33, 1979):113–137, October 1979. ISSN 0066-4227, 1545-3251. doi: 10.1146/annurev.mi.33.100179.000553. URL <https://www.annualreviews.org/content/journals/10.1146/annurev.mi.33.100179.000553>.
- [64] Sergei B. Vakulenko and Shahriar Mobashery. Versatility of Aminoglycosides and Prospects for Their Future. *Clinical Microbiology Reviews*, 16(3):430–450, July 2003. doi: 10.1128/cmr.16.3.430-450.2003. URL <https://journals.asm.org/doi/10.1128/cmr.16.3.430-450.2003>.
- [65] Sophie Leclercq, Firoz M. Mian, Andrew M. Stanisz, Laure B. Bindels, Emmanuel Cambier, Hila Ben-Amram, Omry Koren, Paul Forsythe, and John Bienenstock. Low-dose penicillin in early life induces long-term changes in murine gut microbiota, brain cytokines and behavior. *Nature Communications*, 8:15062, April 2017. ISSN 2041-1723. doi: 10.1038/ncomms15062. URL <https://www.ncbi.nlm.nih.gov/pmc/articles/PMC5382287/>.
- [66] Global action plan on antimicrobial resistance. URL <https://www.who.int/publications/i/item/9789241509763>.
- [67] Christopher R. Grasso, Kaytee L. Pokrzywinski, Christopher Waechter, Taylor Rycroft, Yanyan Zhang, Alyssa Aligata, Michael Kramer, and Anisha Lamsal. A Review of Cyanophage–Host Relationships: Highlighting Cyanophages as a Potential Cyanobacteria Control Strategy. *Toxins*, 14(6):385, June 2022. ISSN 2072-6651. doi: 10.3390/toxins14060385. URL <https://www.mdpi.com/2072-6651/14/6/385>.
- [68] Katelyn M. McKindles, Makayla A. Manes, Jonathan R. DeMarco, Andrew McClure, R. Michael McKay, Timothy W. Davis, and George S. Bullerjahn. Dissolved Microcystin Release Coincident with Lysis of a Bloom Dominated by *Microcystis* spp. in Western Lake Erie Attributed to a Novel Cyanophage. *Applied and Environmental Microbiology*, 86(22):e01397–20, October 2020. doi: 10.1128/AEM.01397-20. URL <https://journals.asm.org/doi/10.1128/aem.01397-20>.

- [69] (PDF) Economic Impacts of Red Tide Events on Restaurant Sales. URL https://www.researchgate.net/publication/23515658_Economic_Impacts_of_Red_Tide_Events_on_Restaurant_Sales.
- [70] Yung Sung Cheng, Yue Zhou, Clinton M. Irvin, Richard H. Pierce, Jerome Naar, Lorraine C. Backer, Lora E. Fleming, Barbara Kirkpatrick, and Dan G. Baden. Characterization of Marine Aerosol for Assessment of Human Exposure to Breve-toxins. *Environmental Health Perspectives*, 113(5):638–643, May 2005. ISSN 0091-6765. doi: 10.1289/ehp.7496. URL <https://www.ncbi.nlm.nih.gov/pmc/articles/PMC1257561/>.
- [71] Barbara Kirkpatrick, Judy A Bean, Lora E Fleming, Gary Kirkpatrick, Lynne Grief, Kate Nierenberg, Andrew Reich, Sharon Watkins, and Jerome Naar. Gastrointestinal Emergency Room Admissions and Florida Red Tide Blooms. *Harmful algae*, 9(1):82–86, January 2010. ISSN 1568-9883. doi: 10.1016/j.hal.2009.08.005. URL <https://www.ncbi.nlm.nih.gov/pmc/articles/PMC2786186/>.
- [72] Porter Hoagland, Di Jin, Lara Y. Polansky, Barbara Kirkpatrick, Gary Kirkpatrick, Lora E. Fleming, Andrew Reich, Sharon M. Watkins, Steven G. Ullmann, and Lorraine C. Backer. The costs of respiratory illnesses arising from Florida gulf coast *Karenia brevis* blooms. *Environmental Health Perspectives*, 117(8):1239–1243, August 2009. ISSN 1552-9924. doi: 10.1289/ehp.0900645.